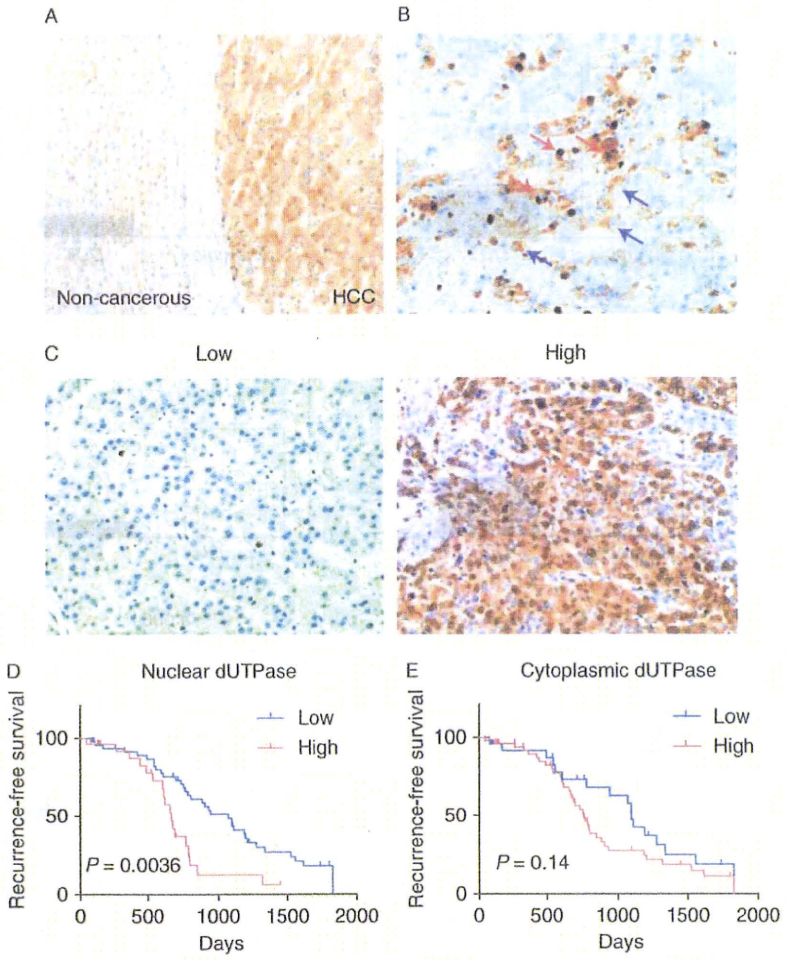

Fig. 3. Immunohistochemistry analysis of dUTP pyrophosphatase (dUTPase) expression in hepatocellular carcinoma (HCC). (A) A representative photomicrograph of dUTPase staining in an HCC and adjacent non-cancerous liver tissue. (B) A representative photomicrograph of dUTPase staining in an HCC. Both nuclear (red arrows) and cytoplasmic (blue arrows) forms of dUTPase were detected. (C) Representative photomicrographs of HCC tissues with low (0–50%) and high (≥ 50%) frequencies of nuclear and cytoplasmic dUTPase-positive cells. (D and E) Kaplan–Meier survival analysis of HCC tissues with nuclear (D) or cytoplasmic (E) dUTPase expression. High percentages of nuclear dUTPase-positive tumour cells significantly correlated with poor clinical outcome in recurrence-free survival.

HCC and nuclear dUTPase expression, implicating the potential effectiveness of nuclear dUTPase level as a biomarker for predicting the survival of HCC patients after surgical resection.

Discussion

Here, using a global gene expression profiling approach (18), we have identified the activation of the nucleotide/nucleoside metabolism-related gene *DUT* (encoding dUTPase) in HCC. Notably, an intense dUTPase expression was detected in a subset of HCC with a poor prognosis. To the best of our knowledge, this is the first report describing the correlation between dUTPase activation and poor survival outcome in HCC patients.

In normal cells, dUTPase is known to catalyse the hydrolysis of dUTP to dUMP in order to maintain the dUMP pool at a certain level for thymidylate synthesis (26). Interestingly, dUTPase mutations in *Escherichia coli* increased dUTP levels, leading to dUTP misincorporation into DNA during replication, which resulted in DNA fragmentation and apoptosis (27). Furthermore, introduction of *E. coli* dUTPase into human tumour cells resulted in the induction of resistance to fluorodeoxyuridine cytotoxicity (28), suggesting a pivotal role of dUTPase in the prevention of DNA damage. Thus, dUTPase activation in the nucleus appears to be critical

Table 2. Clinicopathological characteristics and dUTP pyrophosphatase expression in hepatocellular carcinoma ($n = 82$)

dUTPase expression (nuclear)	Low ($n = 52$)	High ($n = 30$)	*P*-value
Age (< 60 years/≥ 60 years)	19/33	8/22	0.36
Sex (male/female)	36/16	23/7	0.47
Virus (HBV/HCV/B + C/NBNC)	15/33/1/3	10/20/0/0	0.48
Cirrhosis (yes/no)	33/19	22/8	0.36
AFP (< 20 ng/ml/≥ 20 ng/ml)	32/20	15/15	0.31
Histological grade*			
I–II	14	3	
II–III	36	20	
III–IV	2	7	0.0099
Tumour size (< 3 cm/≥ 3 cm)	31/21	19/11	0.74
TNM classification† (I, II/III, IV)	43/9	25/5	0.94
dUTPase expression (cytoplasmic)	**Low ($n = 27$)**	**High ($n = 55$)**	***P*-value**
Age (< 60 years/≥ 60 years)	10/17	17/38	0.58
Sex (male/female)	19/8	40/15	0.82
Virus (HBV/HCV/B + C/NBNC)	8/17/1/1	17/36/0/2	0.56
Cirrhosis (yes/no)	17/10	38/17	0.58
AFP (< 20 ng/ml/≥ 20 ng/ml)	16/11	31/24	0.80
Histological grade*			
I–II	7	10	
II–III	20	36	
III–IV	0	9	0.077
Tumour size (< 3cm/≥ 3 cm)	17/10	33/22	0.80
TNM classification† (I, II/III, IV)	21/6	47/8	0.39

*Edmondson–Steiner grades.
†UICC TNM classification of liver cancer, 6th edition (2002).
AFP, α-fetoprotein; dUTPase, dUTP pyrophosphatase; HBV, hepatitis B virus; HCV, hepatitis C virus.

Table 3. Cox regression analysis of recurrence-free survival rate relative to dUTP pyrophosphatase expression and clinicopathological parameters ($n = 82$)

	Univariate		Multivariate	
Variables (n)	HR (95% CI)	*P*-value	HR (95% CI)	*P*-value
Child–Pugh				
A	1			
B	1.73 (0.50–5.97)	0.38		
Tumour size				
< 3 cm ($n = 50$)	1			
≥ 3 cm ($n = 32$)	1.58 (0.69–3.63)	0.28		
TNM stage*				
I, II ($n = 68$)	1		1	
III, IV ($n = 14$)	2.57 (1.05–6.29)	0.039	2.75 (1.11–6.79)	0.027
Serum AFP				
< 20 ng/ml ($n = 49$)	1			
≥ 20 ng/ml ($n = 38$)	1.54 (0.66–3.56)	0.31		
Microvascular invasion				
No	1			
Yes	1.98 (0.89–4.44)	0.095		
BCLC stage				
A	1			
B/C	2.16 (0.93–5.00)	0.07		
Cytoplasmic dUTPase				
Low ($n = 27$)	1			
High ($n = 55$)	1.15 (0.50–2.62)	0.73		
Nuclear dUTPase				
Low ($n = 52$)	1		1	
High ($n = 30$)	2.47 (1.08–5.66)	0.032	2.61 (1.13–6.05)	0.024

*UICC TNM classification of liver cancer, 6th edition (2002).
AFP, α-fetoprotein; CI, confidence intervals; dUTPase, dUTP pyrophosphatase; HR, hazard ratio.

for preventing DNA damage possibly at the S phase. Specifically, this activation may prevent dUTP misincorporation in various cancers and thus avert DNA damage and apoptosis induction. Indeed, dUTPase activation has recently been reported in colorectal and brain cancer (29, 30), and dUTPase accumulation might correlate with 5-FU-based chemotherapy resistance and poor prognosis in colorectal cancer (26).

If dUTPase activation plays a central role in the development of resistance to thymidylate synthase inhibitors in order to prevent a DNA damage response, dUTPase inhibition may facilitate the eradication of cancer cells by sensitizing these cells to such inhibitors. Indeed, a recent study suggested a drastic sensitization of colon cancer cells to 5-FU by siRNAs-mediated dUTPase suppression (31, 32), which is consistent with our current observation. Because all HCC samples used in this study were surgically resected, we could not evaluate the effect of dUTPase expression on clinical HCC patients' outcome in relation to chemosensitivity to thymidylate synthase inhibitors. Nevertheless, intense nuclear dUTPase expression may be a good biomarker for predicting the response to thymidylate synthase inhibitors, and its usefulness should be further evaluated in the future.

In conclusion, comprehensive gene expression profiling shed new light on the role of dUTPase in HCC. Nuclear dUTPase accumulation is potentially a good biomarker for predicting poor prognosis in HCC patients, and the development of a dUTPase inhibitor may promote the possibility of tumour eradication in HCC patients.

Acknowledgements

The authors would like to thank Ms Masayo Baba and Nami Nishiyama for technical assistance. This research was supported in part by a Grant-in-Aid for Special Purposes from the Ministry of Education, Culture, Sports, Science and Technology, Japan (no. 20599005).

Grant support: Grant-in-Aid for Special Purposes from the Ministry of Education, Culture, Sports, Science and Technology, Japan (no. 20599005).

References

1. Parkin DM, Bray F, Ferlay J, Pisani P. Global cancer statistics, 2002. *CA Cancer J Clin* 2005; **55**: 74–108.
2. El-Serag HB, Rudolph KL. Hepatocellular carcinoma: epidemiology and molecular carcinogenesis. *Gastroenterology* 2007; **132**: 2557–76.
3. Farazi PA, Depinho RA. Hepatocellular carcinoma pathogenesis: from genes to environment. *Nat Rev Cancer* 2006; **6**: 674–87.
4. Roessler S, Budhu A, Wang XW. Future of molecular profiling of human hepatocellular carcinoma. *Future Oncol* 2007; **3**: 429–39.
5. El-Serag HB, Marrero JA, Rudolph L, Reddy KR. Diagnosis and treatment of hepatocellular carcinoma. *Gastroenterology* 2008; **134**: 1752–63.
6. Llovet JM, Bruix J. Novel advancements in the management of hepatocellular carcinoma in 2008. *J Hepatol* 2008; **48**(Suppl. 1): S20–37.
7. Poon RT, Fan ST, Lo CM, Liu CL, Wong J. Long-term survival and pattern of recurrence after resection of small hepatocellular carcinoma in patients with preserved liver function: implications for a strategy of salvage transplantation. *Ann Surg* 2002; **235**: 373–82.
8. Friedman MA. Primary hepatocellular cancer–present results and future prospects. *Int J Radiat Oncol Biol Phys* 1983; **9**: 1841–50.
9. Lin DY, Lin SM, Liaw YF. Non-surgical treatment of hepatocellular carcinoma. *J Gastroenterol Hepatol* 1997; **12**: S319–28.
10. Nagano H, Miyamoto A, Wada H, *et al.* Interferon-alpha and 5-fluorouracil combination therapy after palliative hepatic resection in patients with advanced hepatocellular carcinoma, portal venous tumor thrombus in the major trunk, and multiple nodules. *Cancer* 2007; **110**: 2493–501.
11. Patt YZ, Hassan MM, Lozano RD, *et al.* Phase II trial of systemic continuous fluorouracil and subcutaneous recombinant interferon alfa-2b for treatment of hepatocellular carcinoma. *J Clin Oncol* 2003; **21**: 421–7.
12. Urabe T, Kaneko S, Matsushita E, Unoura M, Kobayashi K. Clinical pilot study of intrahepatic arterial chemotherapy with methotrexate, 5-fluorouracil, cisplatin and subcutaneous interferon-alpha-2b for patients with locally advanced hepatocellular carcinoma. *Oncology* 1998; **55**: 39–47.
13. Obi S, Yoshida H, Toune R, *et al.* Combination therapy of intraarterial 5-fluorouracil and systemic interferon-alpha for advanced hepatocellular carcinoma with portal venous invasion. *Cancer* 2006; **106**: 1990–7.
14. Honda M, Yamashita T, Ueda T, *et al.* Different signaling pathways in the livers of patients with chronic hepatitis B or chronic hepatitis C. *Hepatology* 2006; **44**: 1122–38.
15. Nishino R, Honda M, Yamashita T, *et al.* Identification of novel candidate tumour marker genes for intrahepatic cholangiocarcinoma. *J Hepatol* 2008; **49**: 207–16.
16. Yamashita T, Honda M, Takatori H, *et al.* Genome-wide transcriptome mapping analysis identifies organ-specific gene expression patterns along human chromosomes. *Genomics* 2004; **84**: 867–75.
17. Yamashita T, Kaneko S, Hashimoto S, *et al.* Serial analysis of gene expression in chronic hepatitis C and hepatocellular carcinoma. *Biochem Biophys Res Commun* 2001; **282**: 647–54.
18. Yamashita T, Honda M, Kaneko S. Application of serial analysis of gene expression in cancer research. *Curr Pharm Biotechnol* 2008; **9**: 375–82.
19. Yamashita T, Honda M, Takatori H, *et al.* Activation of lipogenic pathway correlates with cell proliferation and poor prognosis in hepatocellular carcinoma. *J Hepatol* 2009; **50**: 100–10.
20. Velculescu VE, Zhang L, Vogelstein B, Kinzler KW. Serial analysis of gene expression. *Science* 1995; **270**: 484–7.
21. Yamashita T, Hashimoto S, Kaneko S, *et al.* Comprehensive gene expression profile of a normal human liver. *Biochem Biophys Res Commun* 2000; **269**: 110–6.
22. Polyak K, Xia Y, Zweier JL, Kinzler KW, Vogelstein B. A model for p53-induced apoptosis. *Nature* 1997; **389**: 300–5.
23. Misu H, Takamura T, Matsuzawa N, *et al.* Genes involved in oxidative phosphorylation are coordinately upregulated with fasting hyperglycaemia in livers of patients with type 2 diabetes. *Diabetologia* 2007; **50**: 268–77.
24. Longley DB, Harkin DP, Johnston PG. 5-fluorouracil: mechanisms of action and clinical strategies. *Nat Rev Cancer* 2003; **3**: 330–8.
25. Whitfield ML, George LK, Grant GD, Perou CM. Common markers of proliferation. *Nat Rev Cancer* 2006; **6**: 99–106.
26. Ladner RD, Lynch FJ, Groshen S, *et al.* dUTP nucleotidohydrolase isoform expression in normal and neoplastic tissues: association with survival and response to 5-fluorouracil in colorectal cancer. *Cancer Res* 2000; **60**: 3493–503.
27. El-Hajj HH, Zhang H, Weiss B. Lethality of a dut (deoxyuridine triphosphatase) mutation in *Escherichia coli*. *J Bacteriol* 1988; **170**: 1069–75.
28. Canman CE, Radany EH, Parsels LA, *et al.* Induction of resistance to fluorodeoxyuridine cytotoxicity and DNA damage in human tumor cells by expression of *Escherichia coli* deoxyuridinetriphosphatase. *Cancer Res* 1994; **54**: 2296–8.
29. Fleischmann J, Kremmer E, Muller S, *et al.* Expression of deoxyuridine triphosphatase (dUTPase) in colorectal tumours. *Int J Cancer* 1999; **84**: 614–7.
30. Romeike BF, Bockeler A, Kremmer E, *et al.* Immunohistochemical detection of dUTPase in intracranial tumors. *Pathol Res Pract* 2005; **201**: 727–32.
31. Koehler SE, Ladner RD. Small interfering RNA-mediated suppression of dUTPase sensitizes cancer cell lines to thymidylate synthase inhibition. *Mol Pharmacol* 2004; **66**: 620–6.

32. Wilson PM, Fazzone W, Labonte MJ, *et al.* Novel opportunities for thymidylate metabolism as a therapeutic target. *Mol Cancer Ther* 2008; 7: 3029–37.

Supporting Information

Additional Supporting Information may be found in the online version of this article:

Fig. S1. Subcellular localization of genes detected in each SAGE library.

Fig. S2. Microarray analysis of *DUT* and *TS* gene expression in 238 HCC cases publicly available (GSE5975). *DUT* was overexpressed more than 2-fold in 121 of 238 HCC tissues (median: 2.03), whereas *TS* was overexpressed more than 2-fold in 54 of 238 HCC tissues (median: 1.41) compared with the non-cancerous liver tissues.

Fig. S3. (A) Transfection of siRNAs targeting *DUT* (DUT2) decreased *DUT* expression compared with the control (scrambled sequence). Gene expression was evaluated in triplicates 72 hours after transfection (mean ± SD). (B) *DUT* gene knockdown sensitized HuH7 cells to low-dose 5-FU (0.25 mg/ml) (mean ± SD).

Fig. S4. Nuclear and cytoplasmic dUTPase expression and cell proliferation in HCC. PCNA indexes in nuclear dUTPase-high HCC were higher than those in -low HCC with statistical significance ($P = 0.01$). Cytoplasmic dUTPase expression was not associated with PCNA indexes in HCC.

Table S1. A summary of constructed SAGE libraries.

Please note: Wiley-Blackwell is not responsible for the content or functionality of any supporting materials supplied by the authors. Any queries (other than missing material) should be directed to the corresponding author for the article.

CD14$^+$ Monocytes Are Vulnerable and Functionally Impaired Under Endoplasmic Reticulum Stress in Patients With Type 2 Diabetes

Takuya Komura,[1] Yoshio Sakai,[1] Masao Honda,[1] Toshinari Takamura,[1] Kouji Matsushima,[2] and Shuichi Kaneko[1]

OBJECTIVE—Although patients with diabetes suffer from increased infections and a higher incidence of cancer due to impaired immune function, details on diabetes-induced decrease in immunity are lacking. We assessed how immune-mediating peripheral blood mononuclear cells (PBMCs) are affected in diabetes.

RESEARCH DESIGN AND METHODS—From 33 patients with type 2 diabetes and 28 healthy volunteers, we obtained PBMCs and investigated their susceptibility to apoptosis and functional alteration.

RESULTS—In a subpopulation of PBMCs, monocytes derived from patients with diabetes were more susceptible to apoptosis than monocytes from healthy volunteers. Monocytes from patients with diabetes had decreased phagocytotic activity and were less responsive to Toll-like receptor (TLR) ligands, although the expression of TLRs did not differ significantly between the two groups. Furthermore, monocytes from patients with diabetes had a distinctly different gene expression profile compared with monocytes from normal volunteers as assessed with DNA microarray analysis. Specifically, quantitative real-time detection PCR measurements showed an elevated expression of the markers of endoplasmic reticulum (ER) stress in diabetic monocytes, and electron microscopic examination of monocytes revealed morphologic alterations in the ER of cells derived from patients with diabetes. Consistently, the ER stress inducer tunicamycin increased apoptosis of otherwise healthy monocytes and attenuated the proinflammatory responses to TLR ligands.

CONCLUSIONS—These data suggest that monocytes comprise a substantially impaired subpopulation of PBMCs in patients with diabetes and that ER stress is involved in these pathologic changes mechanistically. This implies that the affected monocytes should be investigated further to better understand diabetic immunity. ***Diabetes* 59:634–643, 2010**

Type 2 diabetes is the most frequent metabolic disease and the leading cause of human morbidity and mortality (1,2). Based on epidemiologic data, patients with diabetes are immunocompromised and have an increased incidence of infections in the respiratory tract, urinary tract, and skin (3–5). The high incidence of colorectal, breast, and pancreatic malignancies in patients with diabetes is also considered to be a consequence of diabetes-associated defects in immune function (6,7).

Although studies on immune cells and circulating cytokines have shed some light on this diabetic immunologic phenomenon, conflicting results have been reported and do not adequately explain the perturbed immune function in patients with diabetes. Controversial results concerning the phagocytotic activity of polymorphonuclear neutrophils and monocytes are in part due to differences in the patients themselves, insufficient numbers in the study populations, or inconsistencies in the collection of the cell populations under investigation (8–11). Therefore, further studies are needed to explain the decreased immune function of patients with diabetes.

We previously investigated the gene expression signatures of peripheral blood mononuclear cells (PBMCs) in patients with diabetes and observed transcriptional expression features that were distinct from those of healthy volunteers (12). Apoptosis-related genes were upregulated in the PBMCs of patients with diabetes. Based on this result, we investigated apoptotic activity and immunologic function in PBMCs from patients with type 2 diabetes.

We observed that the CD14$^+$ monocyte fraction was the most affected subpopulation of PBMCs from these patients; these cells were especially vulnerable to apoptosis compared with other cell subpopulations. We also found that CD14$^+$ monocytes demonstrated attenuated phagocytotic activity and deficient Toll-like receptor (TLR) signaling, both of which are important for innate immunity (13,14). Transcriptional analysis and electron microscopic examination of monocytes from patients with diabetes showed evidence of endoplasmic reticulum (ER) stress, which may underlie the functional defects in these cells. Collectively, the data presented herein show that CD14$^+$ monocytes are a vulnerable cell population under ER stress in these patients that could contribute to decreases in immune function in diabetes.

RESEARCH DESIGN AND METHODS

Thirty-three patients with type 2 diabetes (male/female, 15/18; age 62.0 ± 8.6 years; A1C 9.2 ± 2.0%) and 28 healthy volunteers (male/female, 15/13; age 58.2 ± 10.2 years; A1C 5.4 ± 0.7%) were enrolled consecutively for the

From [1]Disease Control and Homeostasis, Kanazawa University, Graduate School of Medical Science, Kanazawa, Japan; and the [2]Department of Molecular Preventive Medicine, School of Medicine, The University of Tokyo, Tokyo, Japan.

Corresponding author: Shuichi Kaneko, skaneko@m-kanazawa.jp.

Received 13 May 2009 and accepted 16 November 2009. Published ahead of print at http://diabetes.diabetesjournals.org on 3 December 2009. DOI: 10.2337/db09-0659.

TABLE 1
Characteristics of the study subjects

	Diabetic patients (n = 33)	Healthy volunteers (n = 28)	P
Age (years)	62.0 ± 8.6	58.2 ± 10.2	NS
Sex (male/female)	15/18	15/13	NS
BMI (kg/m^2)	23.5 ± 4.2	23.6 ± 4.8	NS
White blood cell counts (ml)	4,800 ± 1,700	5,600 ± 1,900	NS
Lymphocytes (%)	23.5 ± 3.5	22.7 ± 2.5	NS
Monocytes (%)	5.2 ± 1.6	6.1 ± 2.3	NS
Hemoglobin (g/dl)	14.1 ± 1.3	13.6 ± 1.6	NS
Total cholesterol (mg/dl)	182 ± 24	180 ± 35	NS
Triglyceride (mg/dl)	138 ± 37	163 ± 33	NS
FPG (mg/dl)	185 ± 38	86 ± 7.4	<0.001
A1C (%)	9.2 ± 2.0	5.4 ± 0.7	<0.001
Diabetic complications (+/−)*	19/14	NA	
Insulin treatment (+/−)	10/23	NA	

Data are means ± SD. *Diabetic complications: nephropathy, neuropathy, retinopathy, macroangiopathy. FPG, fasting plasma glucose; NA, not applicable.

apoptosis assay (Table 1). The groups were not significantly different in terms of their clinical parameters, except for the fasting plasma glucose and A1C levels. The patients with diabetes (n = 16) from whom adequate numbers of monocytes were obtained were enrolled for additional experiments along with 17 other patients with diabetes (male/female, 8/9; age 60.5 ± 7.2 years; A1C 8.8 ± 1.8%) whose clinical profiles fit the diabetic profile (Table 1). Informed consent for this study was obtained from all subjects. The experimental protocol was carried out in accordance with the Declaration of Helsinki.

Isolation of subpopulations of PBMCs and flow cytometric analysis. PBMCs were freshly isolated from heparinized venous blood using Ficoll-Hypaque (Sigma-Aldrich, St. Louis, MO) as previously described (12). CD4$^+$ T-cell and CD14$^+$ monocyte subpopulations were isolated using a magnetic cell sorting system in accordance with the manufacturer's protocol (Miltenyi Biotec, Bergisch Gladbach, Germany). Isolated cells were purified by >90% as measured by flow cytometric analysis using FACSCalibur flow cytometer (BD Biosciences, San Jose, CA). To assess the expression of TLRs on monocytes, PBMCs were incubated with phosphatidylethanolamine (PE)-labeled anti-TLR2, -TLR3, or -TLR4 (eBioscience, San Diego, CA) and fluorescein isothiocyanate (FITC)-labeled anti-CD14 antibodies (BD Biosciences) and analyzed by flow cytometry. Data were analyzed using CELLQuest Software (BD Biosciences).

Quantitative real-time detection PCR. Real-time detection (RTD)-PCR was performed as previously described (15). Briefly, total RNA obtained from cells using a MicroRNA isolation kit (Stratagene, La Jolla, CA) was reverse-transcribed using 1 μg oligo (dT) primer and Super Script II Reverse transcriptase (Invitrogen, Carlsbad, CA). The relative quantities of mRNA expression were analyzed by RTD-PCR using ABI PRISM 7900 HT Sequence Detection System (Applied Biosystems, Foster City, CA). All primer pairs and probes were obtained from the TaqMan assay reagents library. Expression levels of genes were calculated with the $2^{-\Delta\Delta Ct}$ method using either β-actin or GAPDH as internal control genes.

Apoptotic cell detection assay. Freshly isolated PBMCs were incubated with AIM-V (Invitrogen) serum-free culture media containing 5 or 30 mmol/l glucose at 37°C with 5% CO_2 for up to 24 h. The cells were incubated with FITC-labeled anti-CD4, -CD14, or -CD56 antibodies (BD Biosciences) and with PE-labeled annexin-V and 7-amino-actinomycin D (7-AAD) (BD Biosciences) in PBS containing 2% BSA (Sigma-Aldrich). Apoptotic cells were determined by flow cytometry as the fraction of cells labeled with annexin-V that were 7-AAD negative. At least 10,000 cells per sample were analyzed.

Phagocytosis assay. Phagocytotic activity was assessed using a Phagotest Kit (Orpegen Pharma, Heidelberg, Germany) and FITC-labeled opsonized *Escherichia coli* in accordance with the manufacturer's protocol. Briefly, heparinized whole blood obtained from the 33 patients with diabetes and 28 healthy volunteers was incubated with FITC-labeled *E. coli* for 10 min at 37°C. After removing the erythrocytes, the remaining cells were incubated with propidium iodide to detect viable leukocytes by flow cytometry. Monocyte populations were assessed based on cellular granularity and size as side scatter and forward scatter, respectively, and FITC-positive cells were assessed as monocytes with phagocytosed FITC-labeled *E. coli*.

TLR ligand stimuli and expression of proinflammatory cytokine genes. Peptidoglycan (PGN; 1 μg/ml) from *Streptomyces sp.* (Sigma-Aldrich), Poly (I:C) (5 μg/ml; Sigma-Aldrich), and lipopolysaccharide (LPS; 2 μg/ml) from *E. coli* (Sigma-Aldrich), which are TLR2, TLR3, and TLR4 ligands, respectively, were added to monocytes (3×10^5 cells) freshly isolated from the 33 patients and 28 healthy volunteers in AIM-V media. Before and 3 h after incubation, the expression of tumor necrosis factor-α (TNF-α) and interleukin-1β (IL-1β) was analyzed by RTD-PCR.

Analysis of gene expression by DNA microarray. Total RNA was obtained from CD14$^+$ monocytes using MicroRNA isolation kit (Stratagene), and the mRNA was amplified twice using the Amino Allyl MessageAmp aRNA Kit (Ambion, Austin, TX). The reference RNA sample was isolated from CD14$^+$ monocytes from a 30-year-old healthy male volunteer and amplified in the same manner. Amplified mRNA was labeled with cyanin (Cy) 5 or Cy3 (Amersham, Buckinghamshire, U.K.). Equal amounts of the amplified mRNAs were hybridized to an oligo-DNA chip (AceGene Human Oligo Chip 30K; Hitachi Software Engineering, Yokohama, Japan) overnight and washed prior to image scanning.

The fluorescence intensity of each spot on the oligo-DNA chip was obtained using cDNA Microarray Scan Array G (PerkinElmer, Wellesley, MA). The obtained images were quantified using DNAsis array V2.6 software (Hitachi Software Engineering). For normalization, the intensity of each spot with oligo DNA was subtracted from that of spots without oligo DNA in the same block. The spot was validated when the intensity was within the intensity plus or minus a twofold range of SD within each block. By calibrating the median as the base value, the intensities of all spots were adjusted for normalization between Cy5 and Cy3. Hierarchic clustering of gene expression was calibrated using the method described above using BRB Array Tools (http://linus.nci.nih.gov/BRB-ArrayTools.html). The nonfiltered data were log-transformed and applied to the average linkage clustering with centered correlation. For the functional analysis of the 813 upregulated genes, we used GenMAPP (http://www.genmapp.org), a computer program designed for viewing and analyzing genome-scale data on MAPPs representing biological pathways and any other groups of genes.

Electron microscopy. Monocytes obtained from three healthy volunteers and three patients with diabetes were fixed with 2.5% glutaraldehyde and then postfixed in 1% (vol/vol) cacodylate-buffered osmium tetroxide. Samples were dehydrated in a graded series of ethanol, transferred to propylene oxide, and embedded in Epon-Araldite (Sigma-Aldrich). Ultrathin sections were obtained and observed under a Hitachi H-7500 electron microscope (Hitachi High-Technologies, Hitachinaka, Japan).

Caspase-3 assay and enzyme-linked immunosorbent assay (ELISA) of cytokines. Monocytes from a healthy volunteer were harvested and treated with tunicamycin (1 or 5 μg/ml) in AIM-V media. Every 3 h up to 12 h after tunicamycin treatment, we assessed apoptosis by flow cytometry as described above. After 12 h of incubation, the expression levels of BCL-2, C/EBP homologous protein (CHOP), and BiP (immunoglobulin heavy chain binding protein) were assessed by RTD-PCR. The DEVD-cleaving activity of active caspase-3 was measured using labeled Asp-Glu-Val-Asp-p-nitroanilide (DEVD-pNA) as the substrate and the Caspase-3 Colorimetric Assay Kit (Promega, Madison, WI) in accordance the manufacturer's protocol. The pNA light emission was quantified using a microtiter plate reader at a wavelength of 405 nm. In addition, we measured the production of proinflammatory cytokines by RTD-PCR 6 h after treatment of monocytes (3×10^5 cells) with tunicamycin (1 or 5 μg/ml) or the TLR ligands PGN (1 μg/ml), Poly (I:C) (5 μg/ml), and LPS (2 μg/ml). The concentrations of TNF-α, IL-1β, and IL-6 in the culture supernatants were measured using an ELISA kit (eBioscience).

Statistical analysis. Data are expressed as means ± SEM. The Mann-Whitney U test was applied to assess the significant differences between the two groups. Statistical significance was determined as $P < 0.05$, $P < 0.01$, and $P < 0.001$.

RESULTS

Increased apoptosis of CD14$^+$ monocytes from patients with diabetes. We first assessed the frequency of apoptosis in the PBMC fractions from 33 patients with diabetes and 28 nondiabetic healthy volunteers. Apoptosis of the isolated cells was assessed after 3-h incubation in AIM-V serum-free media containing 5 mmol/l glucose (physiological concentration in blood). As shown in Fig. 1A, a significant difference in the frequency of apoptosis was observed in the PBMCs isolated from patients with diabetes and healthy volunteers. Adding serum to AIM-V serum-free media did not affect the difference in apoptosis (data

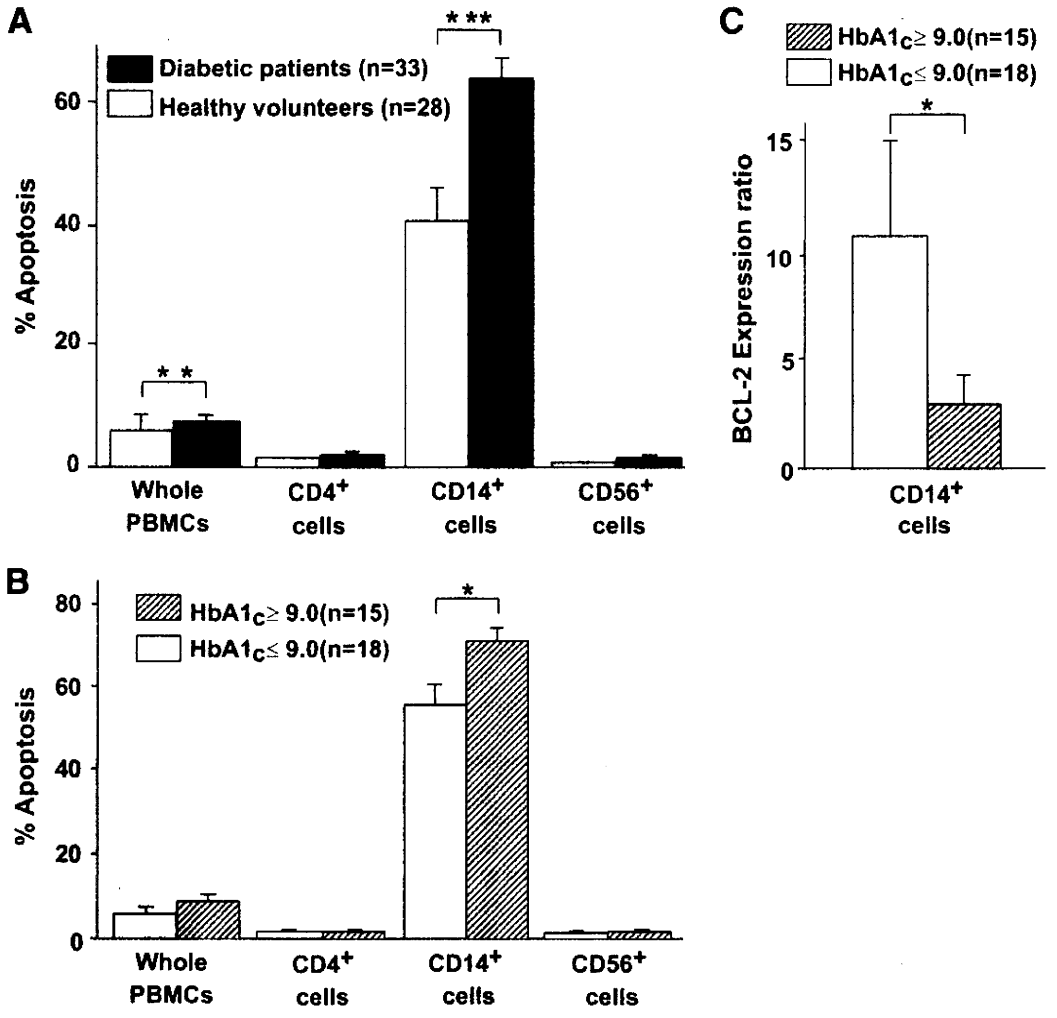

FIG. 1. Monocytes contributed to the vulnerability of the PBMCs in patients with diabetes. *A*: **PBMCs were obtained from 33 patients with diabetes and 28 healthy volunteers. Isolated PBMCs were harvested in AIM-V serum-free culture media supplemented with 5 mmol/l glucose for 3 h and incubated with FITC-labeled anti-CD4, -CD14, or -CD56 antibodies, together with PE-labeled annexin-V to assess the frequency of apoptotic cells in each subpopulation of PBMCs. Apoptotic cells were identified by double-staining with PE-labeled annexin-V and 7-AAD by flow cytometry. The frequencies of apoptotic cells determined as the annexin-V–positive and 7-AAD–negative population are expressed as means ± SEM with statistical comparisons for both groups. The nonparametric Mann-Whitney *U* test was used to calculate the *P* value. ***P* < 0.01, ****P* < 0.001. The PBMCs of patients with diabetes were more susceptible to apoptosis than those of healthy volunteers, and CD14$^+$ monocytes were contributors.** *B*: **Among the 33 patients with diabetes, those with poor glycemic control reflected as A1C ≥9.0% were more susceptible to apoptosis in CD14$^+$ monocytes. Data are expressed as means ± SEM with a statistical comparison of both groups. **P* < 0.05.** *C*: **Monocytes were isolated from 15 patients with A1C ≥9.0% and 18 patients with A1C <9.0%. The expression of the BCL-2 gene in their monocytes before and after incubation in AIM-V serum-free media was assessed by RTD-PCR. After 3-h incubation, the expression of BCL-2 was not upregulated in the poor glycemic control group (A1C ≥9.0%), compared with the fair control group (A1C <9.0%). Data are expressed as means ± SEM with statistical comparisons of both groups. **P* < 0.05.**

not shown). The numbers of whole PBMCs and CD4$^+$, CD14$^+$, and CD56$^+$ cells were similar in both diabetic and healthy subjects (data not shown). CD14$^+$ monocytes were observed to be the major contributor to the increased apoptosis measured in the PBMCs. In contrast, apoptosis of CD4$^+$ T-cells and CD56$^+$ natural killer (NK) cells was not significantly different between the two groups (Fig. 1*A*). When the incubation period in culture media with or without serum was extended to 24 h, ~20% of the CD56$^+$ NK cells of both patients with diabetes and healthy volunteers were induced to undergo apoptosis. When incubation period was extended to 5 days, ~5% of CD4$^+$ T-cells of both patients with diabetes and healthy volunteers were induced to undergo apoptosis; there was no significant difference in cell viability of CD56$^+$ NK cells and CD4$^+$ T-cells between the two groups (data not shown). BCL-2 expression of CD4$^+$ T-cells was not different between the two groups (data not shown). Apoptosis of PBMC subpopulations incubated in culture media containing 30 mmol/l glucose was not different from cells incubated in 5 mmol/l glucose-containing media (data not shown). Moreover, the susceptibility of PBMCs from patients with diabetes to apoptosis was not related to clinical features such as vascular complications, insulin treatment, and fasting plasma glucose concentrations (data not shown).

However, among the 33 patients with diabetes, the frequency of apoptotic CD14$^+$ monocytes from those with poor glycemic control (A1C ≥9.0%) was elevated compared with patients with fair glycemic control (A1C <9.0%) (Fig. 1*B*). Furthermore, after 3-h incubation, the increased ratio of the expression of the antiapoptotic gene, BCL-2, was substantially lower in monocytes from the 15 patients with A1C ≥9.0% compared with the 18

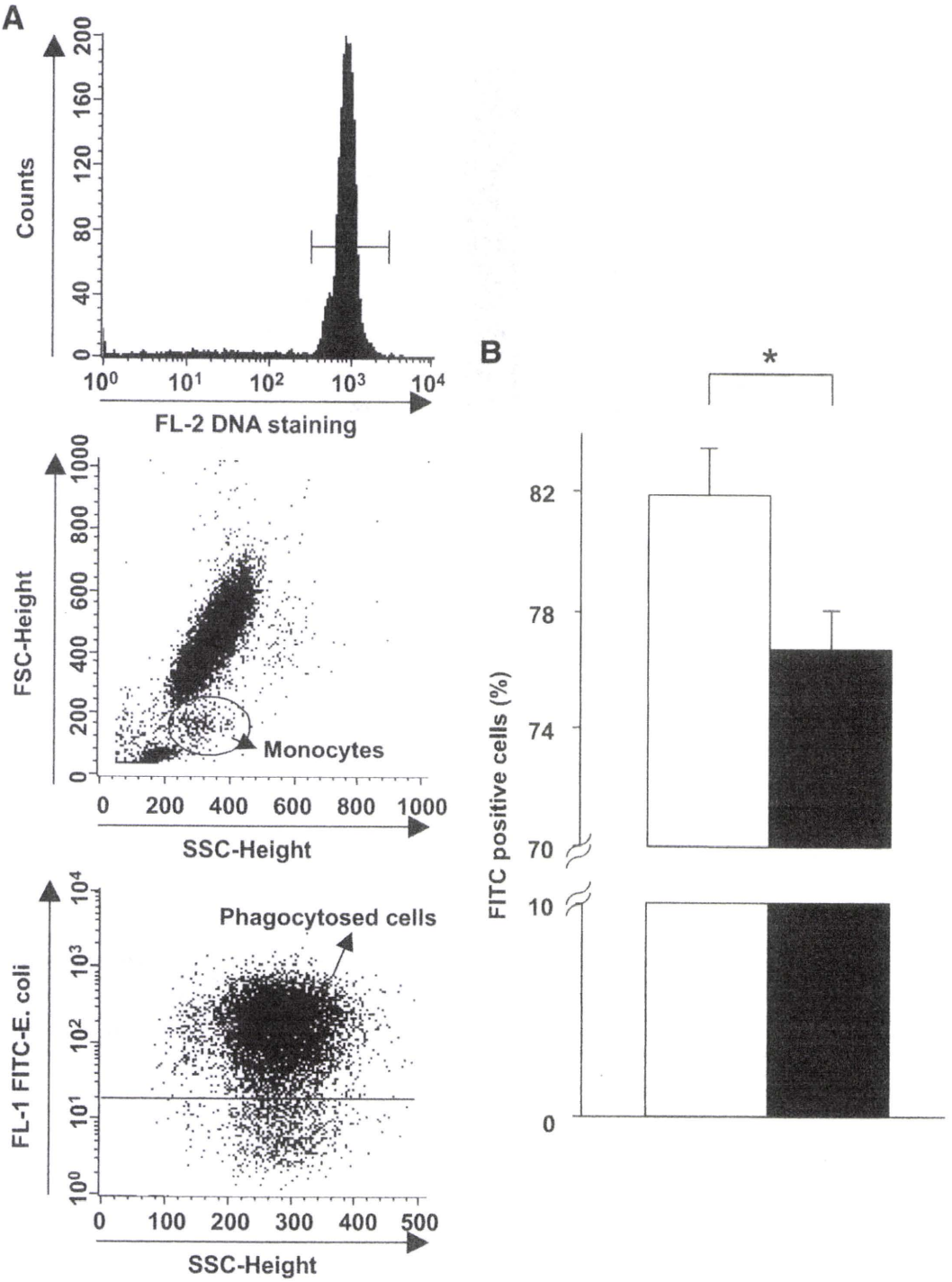

FIG. 2. Attenuated phagocytosis activity in diabetic monocytes. Whole PBMCs were incubated with FITC-labeled *E. coli* for 10 min followed by propidium iodide staining and flow cytometric analysis. *A*: Gated propidium iodide–positive populations were viable leukocyte populations (*upper panel*). The monocyte population was assessed using granularity (side scatter) and size (forward scatter) (*middle panel*). For the gated cells indicating viable monocytes, FITC-positive cells were assessed as monocytes containing phagocytosed FITC-labeled *E. coli* (*lower panel*). *B*: The frequency of monocytes containing phagocytosed *E. coli* in patients with diabetes (■, $n = 33$) was less than that in healthy volunteers (□, $n = 28$). Data are expressed as means ± SEM. $^*P < 0.05$.

patients having A1C <9.0%, as assessed by RTD-PCR (Fig. 1*C*). These data suggest that the monocytes of patients with diabetes are susceptible to apoptosis, especially under conditions of poor glycemic control.

Attenuated function of monocytes from patients with diabetes. To determine whether functional alterations exist in monocytes isolated from the 33 patients with diabetes, we cocultured the monocytes with FITC-labeled *E. coli* and counted the number of fluorescent monocytes that phagocytosed the labeled *E. coli* by flow cytometry. The ratio of monocytes that phagocytosed *E. coli* to all monocytes in patients with diabetes was higher than in the healthy volunteers (Fig. 2*A* and *B*). No significant correlation was observed between the ratio of phagocy-

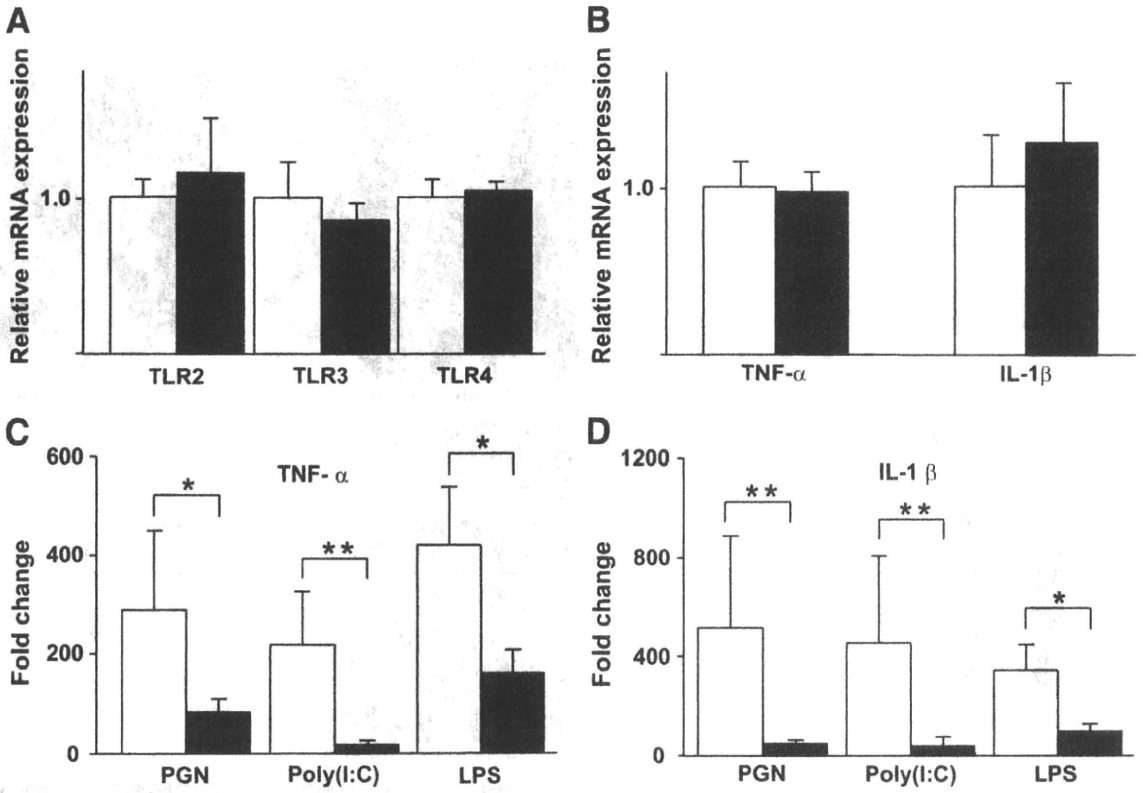

FIG. 3. Hyporesponsiveness to TLR ligand stimuli by the monocytes of patients with diabetes. *A–D*: Isolated CD14$^+$ monocytes from 33 patients with diabetes (■) and 28 healthy volunteers (□) were cultured in AIM-V serum-free media supplemented with each TLR ligand: PGN, Poly (I:C), and LPS. After 3-h incubation, RNA was isolated from the monocytes, and the expression levels of the TNF-α and IL-1β genes were analyzed by RTD-PCR. The basal (prestimuli) expression of TLR2, TLR3, and TLR4 (*A*) and TNF-α and IL-1β (*B*) did not differ significantly between the two groups. The TLR ligand–induced expression of TNF-α (*C*) and IL-1β (*D*) was downregulated in the monocytes of patients with diabetes. Data are expressed as means ± SEM. *$P < 0.05$, **$P < 0.01$.

tosed *E. coli* and A1C levels among the patients (data not shown).

Next, we assessed the responsiveness of monocytes to external pathogenic stimuli in vitro. Monocytes typically express pattern-recognition molecules such as the TLRs that are important for innate immunity against various pathogens (13,14). The expression levels of TLR2, TLR3, and TLR4 were not significantly different between monocytes from patients with diabetes and those from healthy volunteers, as assessed by RTD-PCR (Fig. 3*A*) and flow cytometry (data not shown). We also found that transcriptional expression of TLR signal molecules (MyD88, IRAK1, and TRAF6 for TLR2 and TLR4 signaling and TRIF for TLR3 signaling) was not altered in diabetic monocytes compared with nondiabetic monocytes (data not shown). Next, we exposed the monocytes from the patients with diabetes and healthy volunteers to the TLR ligands, PGN (a TLR2 ligand), Poly (I:C) (a TLR3 ligand), and LPS (a TLR4 ligand) and measured the expression of the proinflammatory cytokine genes, TNF-α and IL-1β. After incubation, the expression of the cytokines was not significantly different between the groups (Fig. 3*B*), but the responsiveness to PGN, Poly (I:C), and LPS was significantly attenuated in monocytes from patients with diabetes compared with those from healthy volunteers as assessed by RTD-PCR (Fig. 3*C* and *D*). These results demonstrate that the monocytes of patients with diabetes are functionally impaired, which implies that they could contribute to immune deficiency in diabetes.

ER stress is a molecular feature of impaired monocytes. To elucidate the molecular features of the diabetic monocytes that were distinctly susceptible to apoptosis, DNA microarray analysis was performed on CD14$^+$ cells isolated from five randomly selected patients with diabetes and five healthy volunteers. These subjects demonstrated clinical features near the median of all study subjects. Unsupervised hierarchic clustering analysis was performed to assess the gene expression profiles of monocytes obtained from patients with diabetes and healthy volunteers; 17,184 filtered genes were evaluated after excluding genes that were not expressed or those with low expression levels that prevented their analysis in 50% of the cases. As shown in Fig. 4*A*, two completely discernible clusters formed between the patients with diabetes and the healthy volunteers.

We identified 813 genes that were upregulated in the monocytes from patients with diabetes compared with those of healthy volunteers ($P < 0.05$, Student t test). Analysis of the biological processes concerning these genes was performed using GenMAPP. The identified genes were shown to be involved in posttranslational protein modification systems occurring in the Golgi apparatus or were involved in ER stress (Table 2 and supplementary Table 1, available in an online appendix at http://diabetes.diabetesjournals.org/cgi/content/full/db09-0659/DC1). The elevated expression of genes related to ER stress, such as CHOP and BiP, was confirmed using RTD-PCR; the expression of these genes was significantly higher in the monocytes from the 33

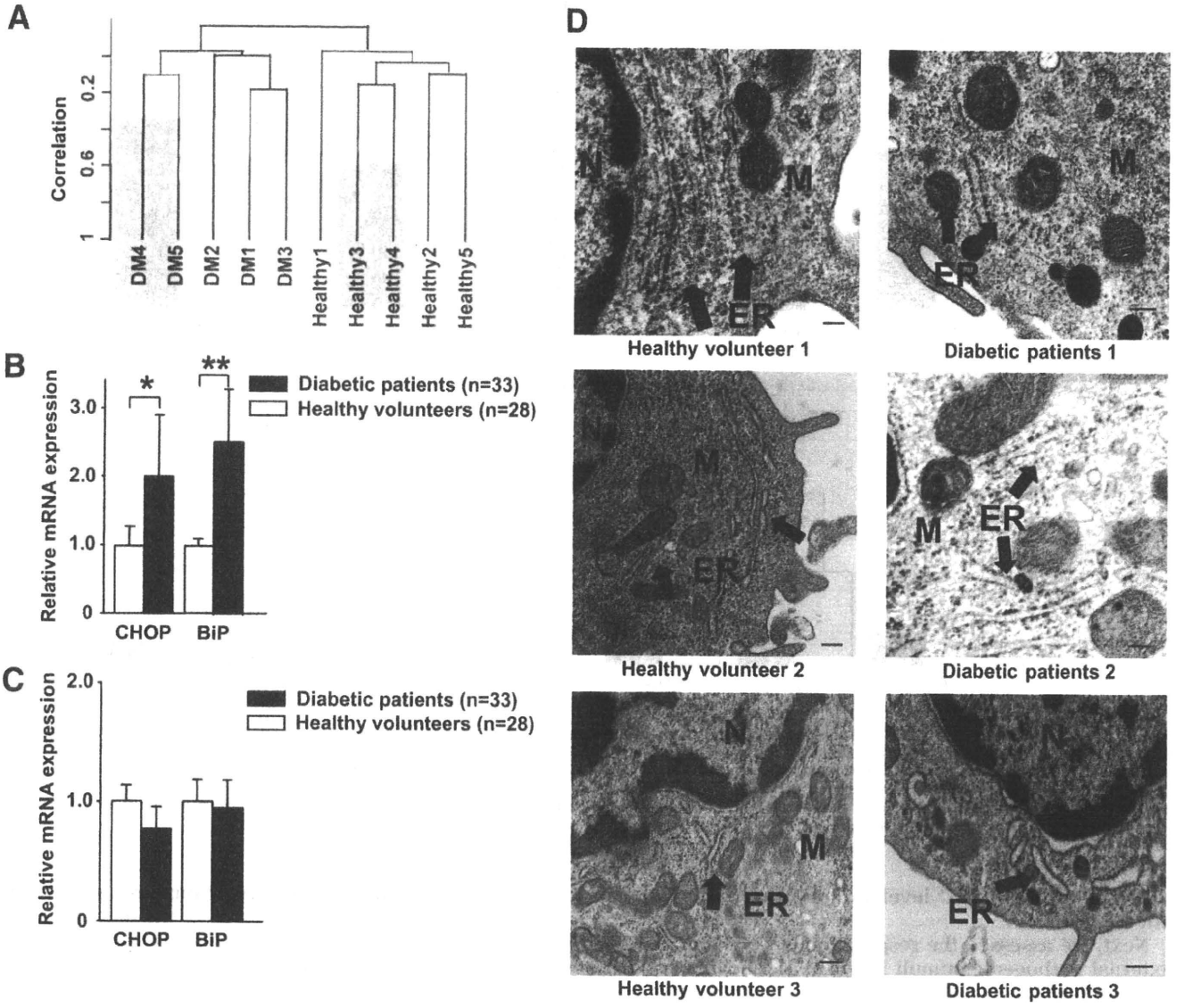

FIG. 4. Monocytes of patients with diabetes were under ER stress. *A*: **The gene expression profiles of representative vulnerable CD14$^+$ monocytes obtained from five patients with diabetes and five healthy volunteers were analyzed using a DNA microarray. Unsupervised hierarchic clustering using 17,184 filtered genes produced two clusters that separated the patients with diabetes from the healthy volunteers without exception.** *B* **and** *C*: **The gene expression levels of the ER stress markers, such as CHOP and BiP, on CD14$^+$ monocytes and CD4$^+$ T-cells obtained from 33 patients with diabetes and 28 healthy volunteers were analyzed using RTD-PCR.** *B*: **The expression levels of CHOP and BiP in monocytes of patients with diabetes were significantly upregulated, compared with the monocytes of healthy volunteers. Data are expressed as means ± SEM. *$P < 0.05$, **$P < 0.01$.** *C*: **The expression levels of CHOP and BiP in T-cells of patients with diabetes were similar to those of healthy volunteers. Data are expressed as means ± SEM.** *D*: **Monocytes were obtained from three healthy volunteers and three patients with diabetes (healthy volunteer 1: 64-year-old man, A1C 5.7%; healthy volunteer 2: 66-year-old man, A1C 4.9%; healthy volunteer 3: 68-year-old woman, A1C 5.6%; diabetic patient 1: 56-year-old man, A1C 9.1%; diabetic patient 2: 64-year-old woman, A1C 8.2%; diabetic patient 3: 71-year-old man, A1C 10.2%) and examined using electron microscopy. In the three patients with diabetes, the concentric, continuous, and regular layer structures of the ER were corrupted, with fewer ribosomes on the ER membrane compared with the ER of the healthy volunteer. ER, endoplasmic reticulum; M, mitochondrion; N, nucleus. Scale bars indicate 100 nm.**

patients with diabetes than in those from the 28 healthy volunteers (Fig. 4*B*). In contrast, no significant difference in the expression of these genes was observed in CD4$^+$ T-cells from patients with diabetes and healthy volunteers (Fig. 4*C*).

Electron microscopy further confirmed ER stress in the monocytes derived from patients with diabetes. As shown in Fig. 4*D*, morphologic alterations of the ER such as corruption of concentric, continuous, and regular layer structure and a decreased number of ribosomes on the ER membrane were evident from the electron photomicrographic images.

ER stress–induced apoptosis and attenuation of TLR signaling in human monocytes. The results described above indicated that the monocytes from patients with diabetes have compromised immunologic function and that ER stress is a distinct feature in these cells. To determine whether ER stress could be a mechanism underlying the observed increase in apoptosis and decreased responsiveness to TLR ligands, CD14$^+$ cells isolated from a healthy volunteer were treated with the ER stress inducer, tunicamycin (1 μg/ml), in AIM-V media. As shown in Fig. 5*A* and *B*, an increased number of apoptotic cells was observed among monocytes treated with tunica-

TABLE 2
Biological processes for upregulated genes in monocytes of diabetic patients

	Z score	Permute *P* value
MAPP name		
Golgi apparatus	3.383	0.000
Ribosomal proteins	3.691	0.002
Unfold protein binding	2.471	0.026
Intracellular protein transport	2.310	0.029
Enzyme-linked receptor protein signaling pathway	2.175	0.042
Nuclear receptor	2.316	0.043
Gametogenesis	−1.998	0.049

mycin compared with untreated monocytes after >6 h of incubation. Treatment of monocytes with a higher concentration of tunicamycin (5 μg/ml) induced more apoptosis (Fig. 5*A* and *B*), and when monocytes were treated with tunicamycin for 12 h, the activity of the proapoptotic protease, caspase-3, significantly increased (Fig. 5*C*). Treatment with tunicamycin coordinately decreased the expression of BCL-2 (Fig. 5*D*) and increased the expression of the ER stress markers, CHOP and BiP (Fig. 5*E*). These results suggest that ER stress promotes apoptosis of human monocytes.

Next, we investigated how tunicamycin-induced ER stress affected the responsiveness of human monocytes to TLR ligands. Treatment of monocytes with tunicamycin for 6 h did not affect the transcriptional and translational expression of TLR2 and TLR4 (data not shown). As shown in Fig. 6*A–C*, however, the expression of the proinflammatory cytokines TNF-α, IL-1β, and IL-6 was downregulated after stimulation with TLR2 and TLR4 ligands. Furthermore, the production of TNF-α, IL-1β, and IL-6 in media was measured by ELISA and found to decrease after treatment of human monocytes with tunicamycin and after stimulation with TLR2 or TLR4 ligands (Fig. 6*D–F*). However, tunicamycin-induced ER stress did not affect expression after treatment of monocytes with the TLR3 ligand, Poly (I:C) (data not shown).

DISCUSSION

In the present study, we observed that PBMCs from patients with diabetes were more susceptible to apoptosis compared with PBMCs from healthy volunteers and that

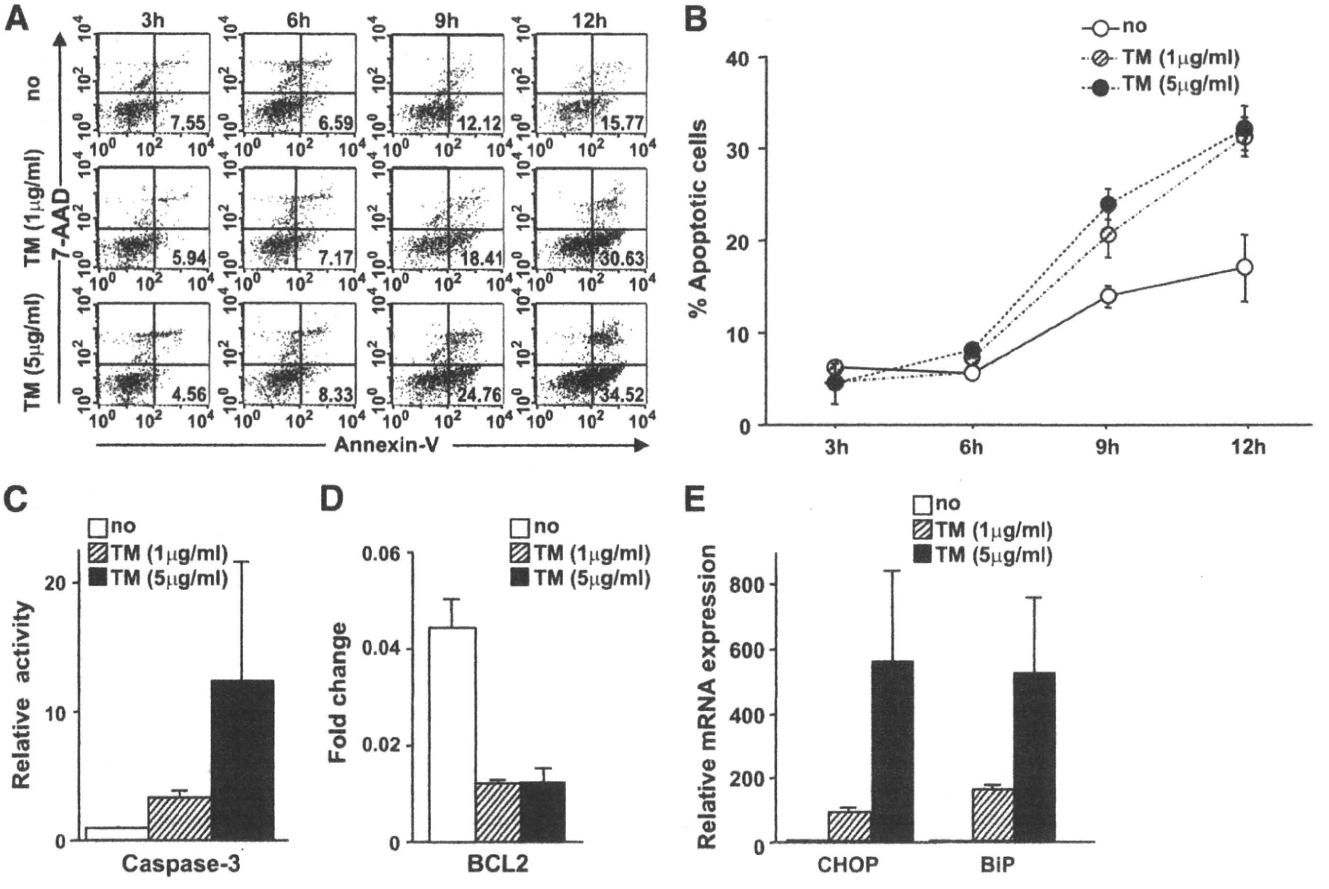

FIG. 5. ER stress enhanced the susceptibility of human monocytes to apoptosis. *A* and *B*: Human CD14$^+$ monocytes obtained from a healthy volunteer were incubated in AIM-V culture media supplemented with tunicamycin (TM) (1 or 5 μg/ml). The frequency of apoptotic cells was analyzed by flow cytometry every 3 h for 12 h. More apoptotic cells were observed among monocytes treated with tunicamycin for >6 h of incubation, compared with untreated monocytes. *A*: Representative scattergram of annexin-V and 7-AAD for monocytes treated with tunicamycin. The numbers in each quadrant indicate the percentage of apoptotic cells. *B*: Apoptotic cells were assessed in triplicate for each condition. Data are expressed as means ± SEM. *C*: Caspase-3 activity in monocytes treated with tunicamycin increased significantly at 12 h of incubation. *D*: The BCL-2 expression in monocytes incubated with tunicamycin for 12 h was downregulated. *E*: The expression levels of the ER stress markers CHOP and BiP in monocytes incubated with tunicamycin for 12 h were significantly upregulated. Data are expressed as means ± SEM of three independent experiments. □, No treatment; ▨, treatment with tunicamycin (1 μg/ml); ■, treatment with tunicamycin (5 μg/ml).

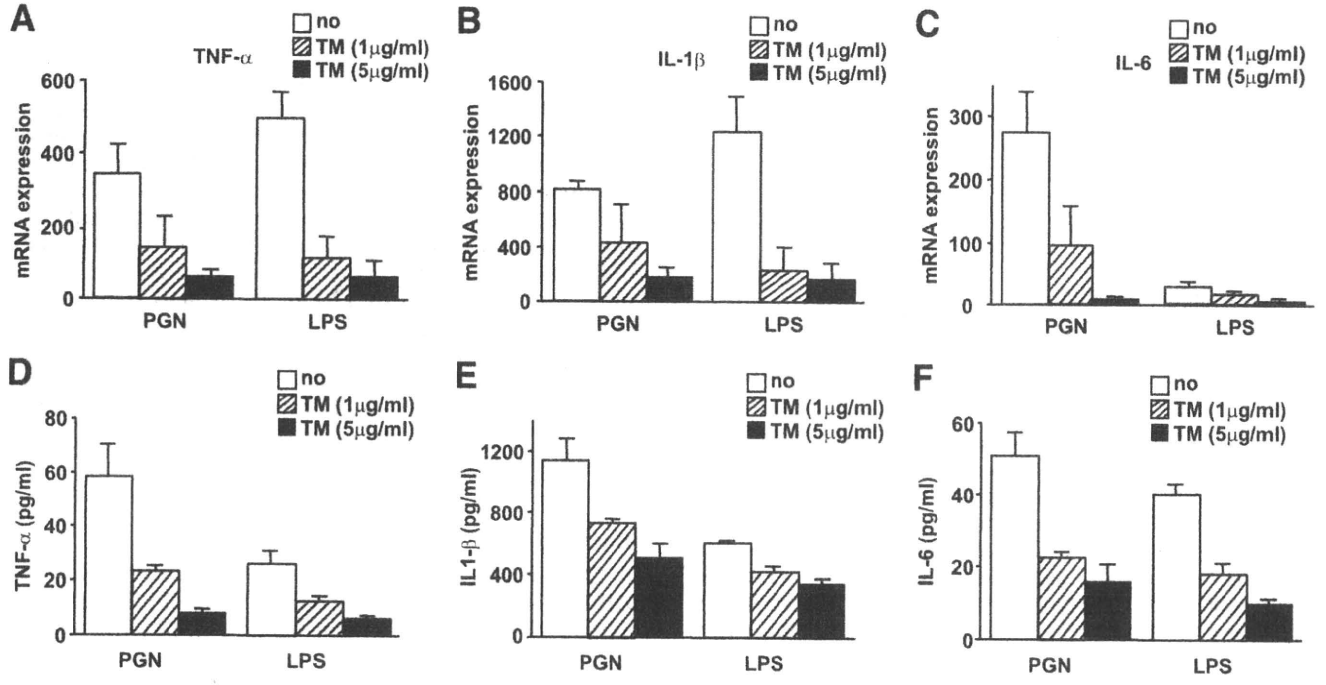

FIG. 6. Expression of proinflammatory cytokines in response to TLR ligand stimuli decreased in human monocytes treated with tunicamycin (TM). Isolated human CD14$^+$ monocytes were incubated in AIM-V culture media with tunicamycin (1 or 5 μg/ml) and stimulated using TLR ligands, PGN, and LPS for 6 h. *A–C*: RTD-PCR analysis showed that the expression of TNF-α (*A*), IL-1β (*B*), and IL-6 (*C*) was downregulated in human CD14$^+$ monocytes treated with tunicamycin, especially at the higher concentration (5 μg/ml). *D–F*: ELISA showed that the production of TNF-α (*D*), IL-1β (*E*), and IL-6 (*F*) in culture media decreased in human monocytes treated with tunicamycin, especially at the higher concentration (5 μg/ml). Data are expressed as means ± SEM of four independent experiments. □, No treatment; ▨, treatment with tunicamycin (1 μg/ml); ■, treatment with tunicamycin (5 μg/ml).

CD14$^+$ monocytes comprised the primary PBMC subpopulation undergoing apoptosis. We also found that CD14$^+$ monocytes from patients with diabetes were hyporesponsive to TLR ligands and that they had attenuated phagocytotic activity. Transcriptional analysis and electron microscopy revealed the presence of ER stress in the affected diabetic monocytes. Consistently, monocytes isolated from nondiabetic patients showed a similar increase in apoptosis and a weakened response to TLR ligands, when they were treated with tunicamycin, indicating that ER stress may be a pivotal mechanism underlying the decreased immunologic function observed in patients with diabetes.

As innate immune-defense mediators, monocytes are capable of ingesting exogenous pathogens to protect the host from infectious diseases. Previous studies have shown that phagocytosis in diabetic neutrophils and monocytes is attenuated (10,11). Similarly, in our study population, monocytes from patients with diabetes were less capable of phagocytosing *E. coli* pathogens compared with monocytes derived from healthy volunteers. This novel finding might explain, at least in part, the decrease in immune function characteristic of patients with diabetes (16). Nevertheless, the detailed mechanisms underlying diabetes-induced decreases in phagocytotic activity remain unclear, because simple high-glucose concentration neither affected the phagocytotic activity and TLR expression nor induced ER stress in nondiabetic monocytes in vitro (data not shown).

The TLRs are pattern-recognition receptors that are important for recognizing pathogens, inducing proinflammatory responses, and preventing the host from acquiring infectious diseases (17–20). The expression of TLR2, TLR3, and TLR4 in CD14$^+$ monocytes was similar between patients with diabetes and healthy volunteers. The administration of a high dose of insulin downregulates TLR expression (21). Transformed monocyte-lineage blastoma cells showed increased TLR expression under hyperglycemic conditions in vitro (22). Type 2 diabetes is characterized as a state of inadequately controlled glycemia associated with hyperinsulinemia due to peripheral insulin resistance (1). Taken together, the TLR expression may be affected by hyperglycemia and hyperinsulinemia in a complex manner. In contrast to the previous finding that monocytes from patients with diabetes were hypersensitive to the TLR ligand, LPS (23,24), we observed that the TNF-α and IL-1β expression from monocytes derived from patients with type 2 diabetes diminished after exposure to PGN, Poly I:C, and LPS—ligands of the TLR2, TLR3, and TLR4 receptors, respectively. These data suggest that diabetes perturbs signaling downstream of the TLRs. In this study, we collected CD14$^+$ monocytes from PBMCs via enrichment using magnetic beads; this protocol was used to remove T-cells, NK cells, B-cells, dendritic cells, and basophils from the PBMC mixture. This is in contrast to the methodology used to isolate these cells in many other studies, in which monocytes were obtained as adherent cells in the culture dish or by a rosetting technique (25,26). CD14$^+$ cells have been shown to be composed of multiple subtypes of activated states; the classical monocyte-isolation methods used in the other studies might unknowingly remove the fraction of monocytes that are susceptible to apoptosis (27). More than half of the CD14$^+$ diabetic monocytes isolated in this study were dead after 12-h incubation, even in media containing physiological concentration of glucose (data not shown).

Our current data showing attenuation of TLR responsiveness to ligands in diabetic monocytes suggest that initial immune responses that are normally triggered by viruses, bacteria, and parasites could be impaired in diabetes, which is consistent with epidemiologic data showing a high incidence of infection in patients with diabetes (3–5).

Gene expression and electron microscopic analysis of monocytes derived from patients with diabetes showed active signatures of ER stress; this is important because ER is an organelle essential for the proper folding and glycosylation of proteins after protein synthesis (28). When cells are under ER stress, protein kinase R–like ER kinase, inositol-requiring enzyme 1, and activating transcription factor 6 are activated and function in the adaptation to stress, proper folding of proteins, and removal of harmful unfolded proteins, respectively (29,30). However, prolonged ER stress leads to apoptotic cell death, which is mediated by CHOP (31). CHOP is a crucial and specific molecule for ER stress–induced apoptosis and alters the transcription of the *BCL-2* gene family members (32). The current study showed that diabetic monocytes had increased levels of ER stress–related apoptotic molecules. Moreover, nondiabetic monocytes treated with tunicamycin, an ER stress inducer, underwent apoptosis in a manner similar to monocytes derived from patients with diabetes. From these data, we conclude that ER stress contributes to the susceptibility of diabetic monocytes to apoptosis.

We also observed that tunicamycin-induced ER stress diminished TLR2 and TLR4 signaling without altering expression of TLRs. Tunicamycin induces ER stress by disturbing N-linked glycosylation (33), and previous reports suggest that perturbations in this glycosylation attenuate TLR2 and TLR4 signaling in vitro (34,35). Hence, these data collectively indicate that ER stress may underlie decreases in TLR2 and TLR4 signaling and affect immune function in patients with diabetes.

TLR3 signaling is different from the other TLR signaling pathway; for example, it is independent of MyD88. TLR2 and TLR4 are expressed on the cell surface, whereas TLR3 is expressed in intracellular compartments such as endosomes (13), and its ligands require internalization before signaling occurs. This suggests that disturbances in TLR3 signaling in diabetic monocytes may be due to reasons other than ER stress. Further investigations are needed to elucidate the detailed mechanisms of attenuated TLR signaling in monocytes from patients with diabetes.

ER stress has been shown to be a mainstay of the diabetic condition. Its pathologic importance in diabetes is especially important in pancreatic β-cells, in which glucose toxicity results in ER stress and insufficient insulin secretion (36–38). The current study suggests that monocytes are yet another population of cells vulnerable to hyperglycemia-induced ER stress and dysfunction. Nevertheless, the mechanisms that render pancreatic β-cells and monocytes vulnerable to ER stress in patients with diabetes remain uncertain.

Diabetes is considered a chronic inflammatory disease. Activated macrophages that produce proinflammatory cytokines such as TNF-α, IL-1β, and IL-6 are thought to contribute to insulin resistance in muscle and adipose tissues (39,40). Furthermore, the atherosclerotic complications in patients with diabetes have a basis in inflammation; local inflammatory foci in atherosclerotic lesions are commonly composed of foam cells derived from activated macrophages (41,42). Further studies are needed to determine whether different subpopulations of monocyte-derived cells, for example, systemically circulating and locally residing inflammatory cells, are susceptible to hyperglycemia-induced ER stress and dysfunction.

In conclusion, our findings show that $CD14^+$ monocytes are susceptible to ER stress–induced alterations in inflammatory signaling and apoptosis, which may play a role in the decreased immune function observed in patients with diabetes. Further investigations are needed to discern the mechanisms of diabetes-induced ER stress and perturbations in inflammatory signaling in $CD14^+$ monocytes.

ACKNOWLEDGMENTS

No potential conflicts of interest relevant to this article were reported.

We thank Dr. Iseki for valuable advice and critical comments on electron microscopic examination about ER of monocytes.

REFERENCES

1. Stumvoll M, Goldstein BJ, van Haeften TW. Type 2 diabetes: principles of pathogenesis and therapy. Lancet 2005;365:1333–1346
2. Zimmet P, Alberti KG, Shaw J. Global and societal implications of the diabetes epidemic. Nature 2001;414:782–787
3. Joshi N, Caputo GM, Weitekamp MR, Karchmer AW. Infections in patients with diabetes mellitus. N Engl J Med 1999;341:1906–1912
4. Shah BR, Hux JE. Quantifying the risk of infectious diseases for people with diabetes. Diabetes Care 2003;26:510–513
5. Finney SJ, Zekveld C, Elia A, Evans TW. Glucose control and mortality in critically ill patients. JAMA 2003;290:2041–2047
6. Dunn GP, Old LJ, Schreiber RD. The immunobiology of cancer immunosurveillance and immunoediting. Immunity 2004;21:137–148
7. Karin M, Lawrence T, Nizet V. Innate immunity gone awry: linking microbial infections to chronic inflammation and cancer. Cell 2006;124:823–835
8. Delamaire M, Maugendre D, Moreno M, Le Goff MC, Allannic H, Genetet B. Impaired leucocyte functions in diabetic patients. Diabet Med 1997;14:29–34
9. Geerlings SE, Hoepelman AI. Immune dysfunction in patients with diabetes mellitus (DM). FEMS Immunol Med Microbiol 1999;26:259–265
10. Katz S, Klein B, Elian I, Fishman P, Djaldetti M. Phagocytotic activity of monocytes from diabetic patients. Diabetes Care 1983;6:479–482
11. Geisler C, Almdal T, Bennedsen J, Rhodes JM, Klendorf K. Monocyte functions in diabetes mellitus. Acta Pathol Microbiol Immunol Scand C 1982;90:33–37
12. Takamura T, Honda M, Sakai Y, Ando H, Shimizu A, Ota T, Sakurai M, Misu H, Kurita S, Matsuzawa-Nagata N, Uchikata M, Nakamura S, Matoba R, Tanino M, Matsubara K, Kaneko S. Gene expression profiles in peripheral blood mononuclear cells reflect the pathophysiology of type 2 diabetes. Biochem Biophys Res Commun 2007;361:379–384
13. Akira S, Uematsu S, Takeuchi O. Pathogen recognition and innate immunity. Cell 2006;124:783–801
14. Pasare C, Medzhitov R. Toll-like receptors: linking innate and adaptive immunity. Microbes Infect 2004;6:1382–1387
15. Tateno M, Honda M, Kawamura T, Honda H, Kaneko S. Expression profiling of peripheral-blood mononuclear cells from patients with chronic hepatitis C undergoing interferon therapy. J Infect Dis 2007;195:255–267
16. Stuart LM, Ezekowitz RA. Phagocytosis and comparative innate immunity: learning on the fly. Nat Rev Immunol 2008;8:131–141
17. Thoma-Uszynski S, Stenger S, Takeuchi O, Ochoa MT, Engele M, Sieling PA, Barnes PF, Rollinghoff M, Bolcskei PL, Wagner M, Akira S, Norgard MV, Belisle JT, Godowski PJ, Bloom BR, Modlin RL. Induction of direct antimicrobial activity through mammalian toll-like receptors. Science 2001;291:1544–1547
18. Barton GM, Medzhitov R. Toll-like receptor signaling pathways. Science 2003;300:1524–1525
19. Sabroe I, Parker LC, Dower SK, Whyte MK. The role of TLR activation in inflammation. J Pathol 2008;214:126–135
20. Iwasaki A, Medzhitov R. Toll-like receptor control of the adaptive immune responses. Nat Immunol 2004;10:987–995
21. Ghanim H, Mohanty P, Deopurkar R, Sia CL, Korzeniewski K, Abuaysheh S, Chaudhuri A, Dandona P. Acute modulation of Toll-like receptors by insulin. Diabetes Care 2008;31:1827–1831

22. Dasu MR, Devaraj S, Zhao L, Hwang DH, Jialal I. High glucose induces toll-like receptor expression in human monocytes: mechanism of activation. Diabetes 2008;57:3090–3098
23. Desfaits AC, Serri O, Renier G. Normalization of plasma lipid peroxides, monocyte adhesion, and tumor necrosis factor-alpha production in NIDDM patients after gliclazide treatment. Diabetes Care 1998;21:487–493
24. Ohno Y, Aoki N, Nishimura A. In vitro production of interleukin-1, interleukin-6, and tumor necrosis factor-alpha in insulin-dependent diabetes mellitus. J Clin Endocrinol Metab 1993;77:1072–1077
25. Renier G, Mamputu JC, Serri O. Benefits of gliclazide in the atherosclerotic process: decrease in monocyte adhesion to endothelial cells. Metabolism 2003;52:13–18
26. Serbina NV, Jia T, Hohl TM, Pamer EG. Monocyte-mediated defense against microbial pathogens. Annu Rev Immunol 2008;26:421–452
27. Wahl LM, Wahl SM, Smythies LE, Smith PD. Isolation of human monocyte populations. Curr Protoc Immunol 2006;Chapter 7:Unit 7.6A
28. Ron D, Walter P. Signal integration in the endoplasmic reticulum unfolded protein response. Nat Rev Mol Cell Biol 2007;8:519–529
29. Xu C, Bailly-Maitre B, Reed JC. Endoplasmic reticulum stress: cell life and death decisions. J Clin Invest 2005;115:2656–2664
30. Bukau B, Weissman J, Horwich A. Molecular chaperones and protein quality control. Cell 2006;125:443–451
31. Wang XZ, Ron D. Stress-induced phosphorylation and activation of the transcription factor CHOP (GADD153) by p38 MAP Kinase. Science 1996;272:1347–1349
32. McCullough KD, Martindale JL, Klotz LO, Aw TY, Holbrook NJ. Gadd153 sensitizes cells to endoplasmic reticulum stress by down-regulating Bcl2 and perturbing the cellular redox state. Mol Cell Biol 2001;21:1249–1259
33. Kataoka H, Yasuda M, Iyori M, Kiura K, Narita M, Nakata T, Shibata K. Roles of N-linked glycans in the recognition of microbial lipopeptides and lipoproteins by TLR2. Cell Microbiol 2006;8:1199–1209
34. Ohnishi T, Muroi M, Tanamoto K. N-linked glycosylations at Asn(26) and Asn(114) of human MD-2 are required for toll-like receptor 4-mediated activation of NF-kappaB by lipopolysaccharide. J Immunol 2001;167:3354–3359
35. Weber AN, Morse MA, Gay NJ. Four N-linked glycosylation sites in human toll-like receptor 2 cooperate to direct efficient biosynthesis and secretion. J Biol Chem 2004;279:34589–34594
36. Ozcan U, Cao Q, Yilmaz E, Lee AH, Iwakoshi NN, Ozdelen E, Tuncman G, Görgün C, Glimcher LH, Hotamisligil GS. Endoplasmic reticulum stress links obesity, insulin action, and type 2 diabetes. Science 2004;306:457–461
37. Oyadomari S, Takeda K, Takiguchi M, Gotoh T, Matsumoto M, Wada I, Akira S, Araki E, Mori M. Nitric oxide-induced apoptosis in pancreatic beta cells is mediated by the endoplasmic reticulum stress pathway. Proc Natl Acad Sci U S A 2001;98:10845–10850
38. Schenk S, Saberi M, Olefsky JM. Insulin sensitivity: modulation by nutrients and inflammation. J Clin Invest 2008;118:2992–3002
39. Kahn SE, Hull RL, Utzschneider KM. Mechanisms linking obesity to insulin resistance and type 2 diabetes. Nature 2006;444:840–846
40. Wellen KE, Hotamisligil GS. Inflammation, stress, and diabetes. J Clin Invest 2005;115:1111–1119
41. Brownlee M. Biochemistry and molecular cell biology of diabetic complications. Nature 2001;414:813–820
42. Liang CP, Han S, Senokuchi T, Tall AR. The macrophage at the crossroads of insulin resistance and atherosclerosis. Circ Res 2007;100:1546–1555

Differential MicroRNA Expression Between Hepatitis B and Hepatitis C Leading Disease Progression to Hepatocellular Carcinoma

Shunsuke Ura,[1] Masao Honda,[1,2] Taro Yamashita,[1] Teruyuki Ueda,[1] Hajime Takatori,[1] Ryuhei Nishino,[1] Hajime Sunakozaka,[1] Yoshio Sakai,[1] Katsuhisa Horimoto,[3] and Shuichi Kaneko[1]

MicroRNA (miRNA) plays an important role in the pathology of various diseases, including infection and cancer. Using real-time polymerase chain reaction, we measured the expression of 188 miRNAs in liver tissues obtained from 12 patients with hepatitis B virus (HBV)-related hepatocellular carcinoma (HCC) and 14 patients with hepatitis C virus (HCV)-related HCC, including background liver tissues and normal liver tissues obtained from nine patients. Global gene expression in the same tissues was analyzed via complementary DNA microarray to examine whether the differentially expressed miRNAs could regulate their target genes. Detailed analysis of the differentially expressed miRNA revealed two types of miRNA, one associated with HBV and HCV infections (n = 19), the other with the stage of liver disease (n = 31). Pathway analysis of targeted genes using infection-associated miRNAs revealed that the pathways related to cell death, DNA damage, recombination, and signal transduction were activated in HBV-infected liver, and those related to immune response, antigen presentation, cell cycle, proteasome, and lipid metabolism were activated in HCV-infected liver. The differences in the expression of infection-associated miRNAs in the liver correlated significantly with those observed in Huh7.5 cells in which infectious HBV or HCV clones replicated. Out of the 31 miRNAs associated with disease state, 17 were down-regulated in HCC, which up-regulated cancer-associated pathways such as cell cycle, adhesion, proteolysis, transcription, and translation; 6 miRNAs were up-regulated in HCC, which down-regulated anti-tumor immune response. *Conclusion:* miRNAs are important mediators of HBV and HCV infection as well as liver disease progression, and therefore could be potential therapeutic target molecules. (HEPATOLOGY 2009;49:1098-1112.)

MicroRNA (miRNA) is an endogenous, small, single-strand, noncording RNA consisting of 20 to 25 bases and regulates gene expression of various cell types. It plays an important role in various biological processes, including organ development and differentiation as well as cellular death and proliferation, and is also involved in various diseases such as infection and cancer.[1-3]

miRNAs are produced as follows. A primary miRNA with a hairpin loop structure is cleaved into a precursor miRNA and transported out of the nuclei with a carrier protein (Exportin-5). The precursor miRNA is then processed by Dicer and converted into an active single-strand RNA in the cytoplasm. The miRNA binds to a target messenger RNA in a sequence-dependent manner and induces degradation of the target messenger RNA and translational inhibition. One miRNA regulates the expression of multiple target genes; bioinformatics analyses have suggested that the expression of more than 30% of human genes is regulated by miRNAs.[4-7]

Abbreviations: cDNA, complementary DNA; CH, chronic hepatitis; CH-B, chronic hepatitis B; CH-C, chronic hepatitis C; HBV, hepatitis B virus; HCC, hepatocellular carcinoma; HCC-B, hepatitis B-related hepatocellular carcinoma; HCC-C, hepatitis C-related hepatocellular carcinoma; HCV, hepatitis C virus; miRNA, microRNA; RTD-PCR, real-time detection polymerase chain reaction; SVM, support vector machine.

From the Departments of [1]Gastroenterology and [2]Advanced Medical Technology, Kanazawa University Graduate School of Medicine, Kanazawa, Japan; and the [3]Biological Network Team, Computational Biology Research Center, National Institute of Advanced Industrial Science and Technology, 2-42 Aomi, koto-ku, Tokyo 135-0064, Japan.

Received July 3, 2008; accepted November 15, 2008.

Address reprint requests to: Masao Honda, M.D., Ph.D., Department of Gastroenterology, Graduate School of Medicine, Kanazawa University, Takara-Machi 13-1, Kanazawa 920-8641, Japan. E-mail: mhonda@m-kanazawa.jp; fax: (81)-76-234-4250.

Published online in Wiley InterScience (www.interscience.wiley.com).

DOI 10.1002/hep.22749

Potential conflict of interest: Nothing to report.

Additional Supporting Information may be found in the online version of this article.

Table 1. Characteristics of Patients Used for Analysis of miRNA and Microarray Samples

Patient No.	Virus	Age	Sex	ALT	Histology of Activity	Background Liver Fibrosis	Histological Grade of HCC	Tumor Size (mm)	TNM Staging	HCV-RNA (KIU/mL)	HBV-DNA (LEG/mL)
1	HBV	57	M	16	2	4	Moderate	20	II	–	3.4
2	HBV	51	M	57	1	2	Moderate	48	II	–	< 2.6
3	HBV	61	M	17	1	4	Well	16	II	–	< 3.7
4	HBV	47	M	19	1	4	Moderate	15	I	–	< 3.7
5	HBV	72	M	19	1	1	Well	25	II	–	NA
6	HBV	73	M	62	1	3	Moderate	45	III	–	5.7
7	HBV	42	M	36	1	4	Moderate	18	I	–	< 3.7
8	HBV	63	M	13	1	2	Moderate	15	I	–	2.8
9	HBV	68	F	54	1	2	Well	56	II	–	4.1
10	HBV	70	M	13	0	2	Well	40	II	–	< 3.7
11	HBV	58	M	29	1	4	Moderate	35	IVA*	–	3.3
12	HBV	72	M	22	1	4	Moderate	18	I	–	6
13	HCV	66	F	33	2	4	Well	25	II	423	–
14	HCV	67	M	89	1	4	Well	30	II	> 850	–
15	HCV	64	M	31	1	4	Moderate	75	III	< 5 (+)	–
16	HCV	68	M	30	0	4	Well	23	II	> 850	–
17	HCV	46	M	98	2	3	Moderate	20	I	> 850	–
18	HCV	68	F	32	2	4	Moderate	25	III	< 5 (+)	–
19	HCV	66	F	46	2	4	Well	25	II	> 850	–
20	HCV	47	M	246	1	3	Moderate	20	I	262	–
21	HCV	75	M	27	1	3	Moderate	19	II	85.1	–
22	HCV	77	M	21	0	1	Moderate	20	II	< 5 (−)	–
23	HCV	66	M	46	2	2	Well	60	II	50.3	–
24	HCV	65	M	89	1	1	Poorly	25	III	850	–
25	HCV	53	M	54	0	1	Moderate	28	II	< 5 (−)	–
26	HCV	75	F	212	1	4	Well	19	I	580	–
27	–	51	F	18	0	0	–	–	–	–	–
28	–	78	F	13	0	0	–	–	–	–	–
29	–	75	M	20	0	0	–	–	–	–	–
30	–	34	M	12	0	0	–	–	–	–	–
31	–	64	M	30	0	0	–	–	–	–	–
32	–	78	M	9	0	0	–	–	–	–	–
33	–	53	M	19	0	0	–	–	–	–	–
34	–	64	F	12	0	0	–	–	–	–	–
35	–	60	F	20	0	0	–	–	–	–	–

HCV RNA was assayed via Amplicor Monitor Test (KIU/mL); HBV DNA was assayed via transcription-mediated amplification (LEG/mL).

Abbreviations: ALT, alanine aminotransferase; F, female; HBV, hepatitis B virus; HCC, hepatocellular carcinoma; HCV, hepatitis C virus; M, male; TNM, tumor-node–metastasis.

*Vascular invasion (+).

Infection of the human liver with hepatitis B virus (HBV) and hepatitis C virus (HCV) induces the development of chronic hepatitis (CH), cirrhosis, and in some instances hepatocellular carcinoma (HCC).[8] The virological features of these two distinct viruses are completely different; however, the viruses infect the liver and cause CH, which is not distinguished by histological examination or clinical manifestations. We previously reported that gene expression profiles in chronic hepatitis B (CH-B) and chronic hepatitis C (CH-C) are different. Proapoptotic and DNA repair responses were predominant in CH-B, and inflammatory and antiapoptotic phenotypes were predominant in CH-C. However, factors inducing these differences in gene expression remain to be elucidated.[9,10]

We examined miRNA expression in liver tissue with HBV-related liver disease (CH-B and HCC-B) and HCV-related liver disease (CH-C and HCC-C) and in normal liver tissue via real-time detection polymerase chain reaction (RTD-PCR). We also performed global analysis of messenger RNA expression in these tissues using complementary DNA (cDNA) microarray. These analyses allowed us to find characteristic miRNAs associated with HBV or HCV infection as well as the progression of liver disease.

Patients and Methods

Patients. The study subjects included 12 patients with CH-B complicated by HCC and 14 patients with

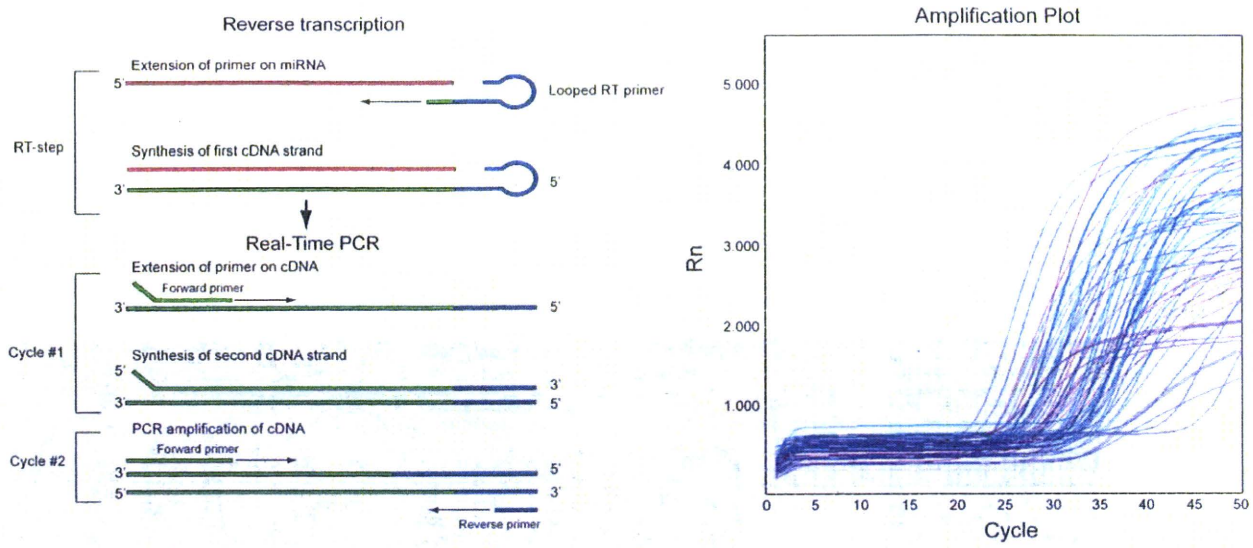

Fig. 1. (A) miRNA-specific RTD-PCR using sheet hairpin primers. (B) miRNA amplification curves by RTD-PCR.

CH-C complicated by HCC. Gene expression analysis was approved by the ethics committee of the Graduate School of Medicine, Kanazawa University Hospital, Japan, between 1999 and 2004. In addition, nine normal liver tissue samples obtained during surgery for metastatic liver cancer were used as control samples. Surgically removed liver tissues were stored in liquid nitrogen until analysis. Histological classification of HCC and histological evaluation of hepatitis in noncancerous regions for each patient are shown in Table 1. HCV viremia in two patients with CH-C was persistently cleared by interferon therapy before HCC development. There were no significant differences in the histological findings of HCC and noncancerous regions, as well as in sex, age, and hepatic function between the HBV and HCV infection groups.

Quantitative RTD-PCR. Approximately 1 mg of each liver tissue sample stored in liquid nitrogen was ground with a homogenizer while still frozen, and total RNA containing miRNA was isolated according to the protocol of the mirVana miRNA Isolation kit (Ambion, Austin, TX) and stored at −80°C until analysis. miRNA expression levels were quantitated using the TaqMan MicroRNA Assays Human Panel Early Access kit (Applied Biosystems, Foster City, CA). cDNA was prepared via reverse transcription using 10 ng each of the isolated total RNA and 3 μL each of the reverse transcription primers with specific loop structures. Reverse transcription was performed using the TaqMan MicroRNA Reverse Transcription kit (Applied Biosystems) according to the manufacturer's protocol. Then, a mixture of 6.67 μL of nuclease-free water, 10 μL of TaqMan 2 × Universal PCR Master Mix (No AmpErase UNG; Applied Biosystems), and 2 μL of TaqMan MicroRNA Assay Mix, which was included in the kit, was prepared for each sample on a 384-well plate; 1.33 μL of the reverse transcription product was added to the mixture, and amplification reaction was performed on an ABI PRISM 7900HT (Applied Biosystems). Expression levels of 188 miRNAs in each sample were quantitated.

Analysis of RTD-PCR Data. The measured 188 miRNAs included RNU6B, which is commonly used as a control for miRNA. β-Actin and glyceraldehyde 3-phosphate dehydrogenase were also measured simultaneously for correcting RNA amount. The mean Ct values and standard deviations of each miRNA were calculated from expression data of all patients obtained by RTD-PCR. miRNA with the lowest expression variation was used as the internal control. Ct values of each miRNA were then corrected by the Ct value of the internal control to yield $-\Delta Ct$ values defined as relative miRNA expression levels and used for analyses. Statistical analyses and hierarchical cluster analyses of expression data were performed using BRB ArrayTools (http://linus.nci.nih.gov/BRB-ArrayTools.html). Relative miRNA expression levels were further normalized using the median over the all patients so that the normalized expression levels of each patient have a median log ratio of 0. A class prediction method was used for classifying two patient groups based on the supervised learning method, and a binary tree classification method was used for classifying three or more patient groups with a statistical algorithm of the support vector machine (SVM). Class prediction was performed using SVM incorporating genes differentially expressed at a univariate parametric significance level of $P = 0.01$. The prediction rate was estimated via cross-validation and the bootstrap method for small sample data.[11] (It is worth

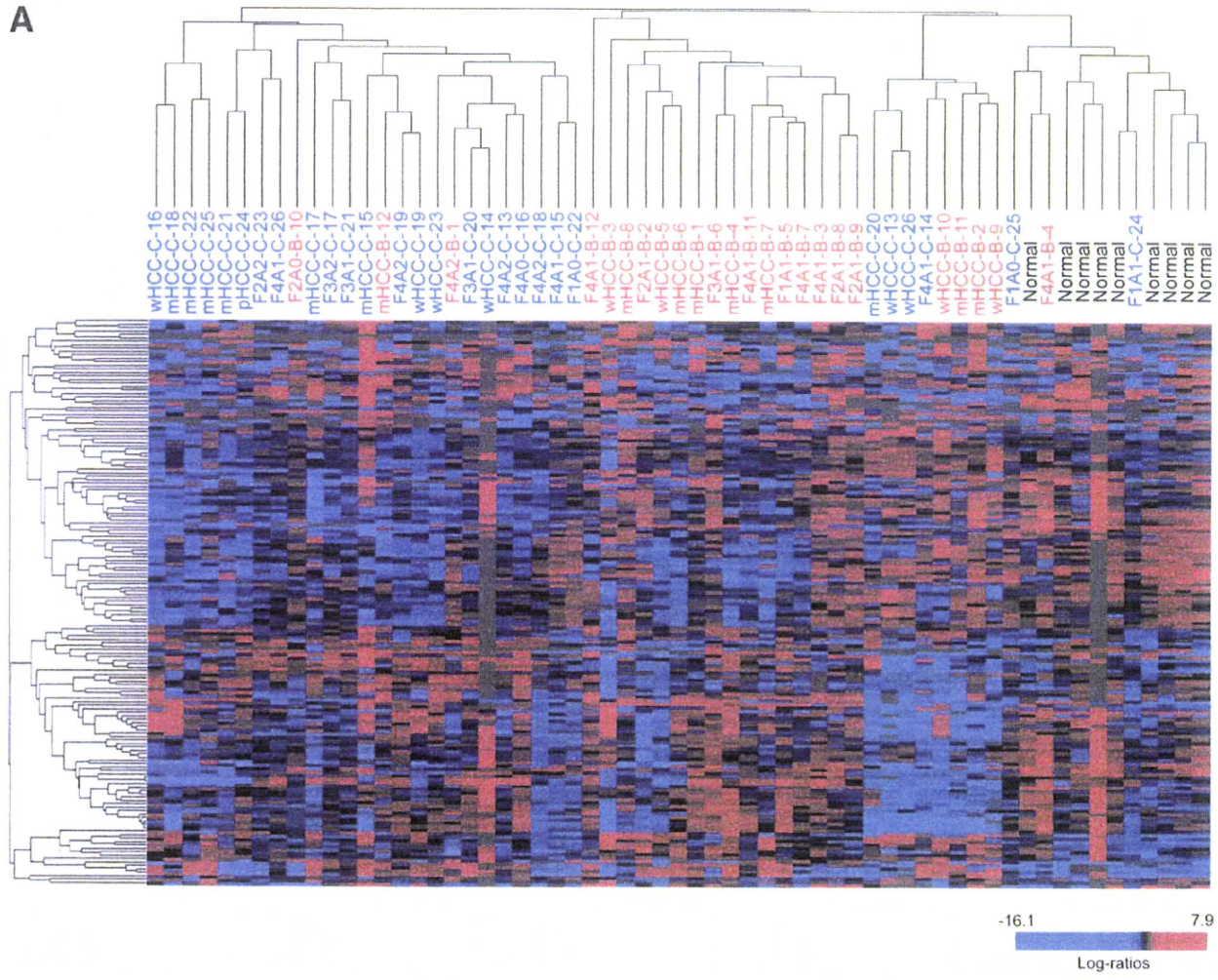

Fig. 2. (A) Hierarchical cluster analysis using total miRNA. Chronic hepatitis is indicated by histological stage and grade (F, fibrosis; A, activity) and type of infecting virus (B or C). HCC is indicated by histological grade (w, well differentiated; m, moderately differentiated; p, poorly differentiated) and type of infecting virus (B or C), with the patient number added at the end. (B) Relationship between five classes divided by binary tree classification. Expression profiles were first classified into normal liver and non-normal liver groups (node 1), then into HBV and HCV groups (node 2). The HBV group was further divided into HCC-B and CH-B (node 3), and the HCV group into HCC-C and CH-C (node 4).

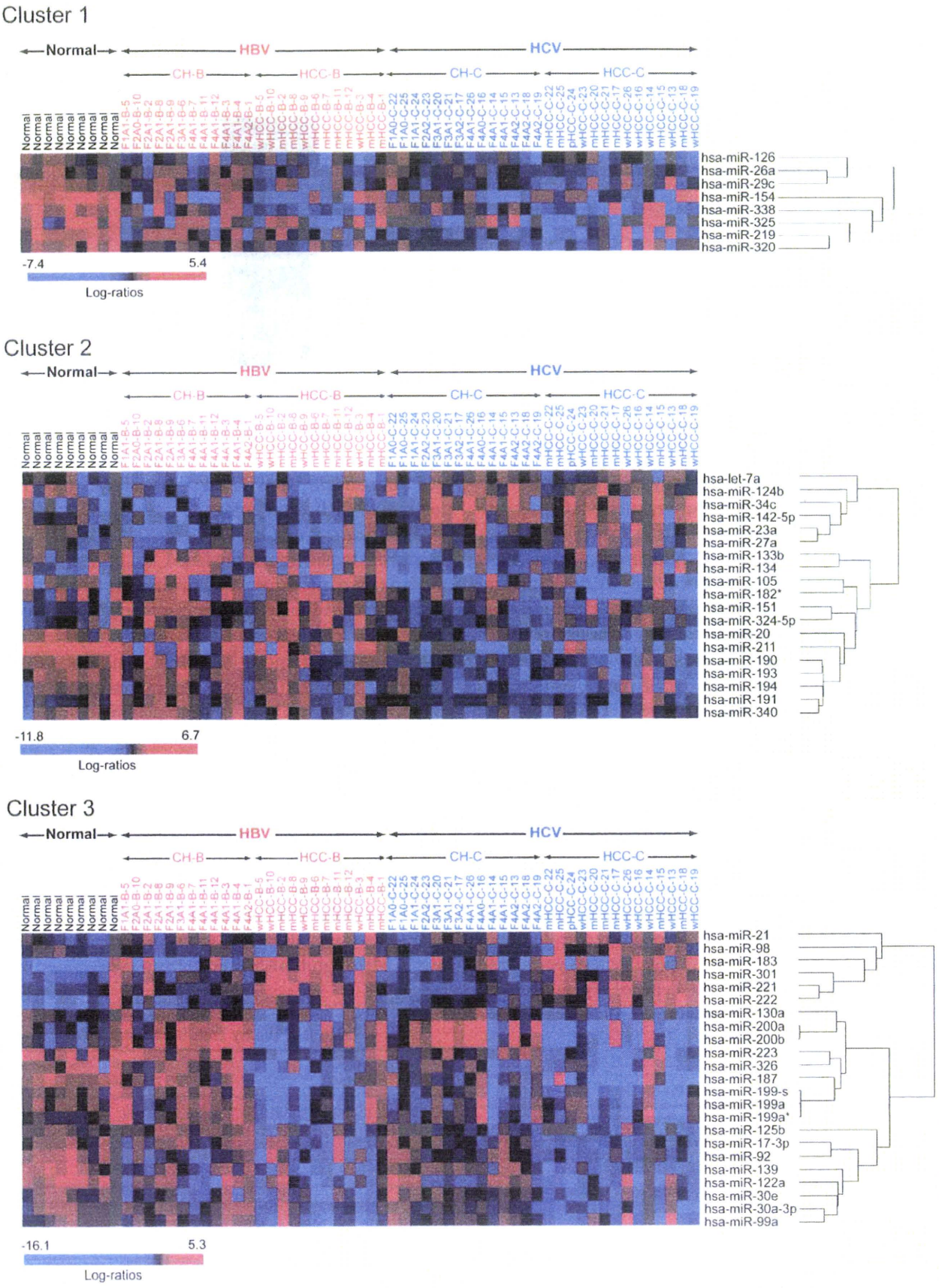

Fig. 3. Cluster 1: Eight miRNAs specifically differentiated node 1 classification. Cluster 2: Nineteen miRNAs specifically differentiated node 2 classification. Cluster 3: Twenty-three miRNAs differentiated CH-B and HCC-B as well as CH-C and HCC-C.

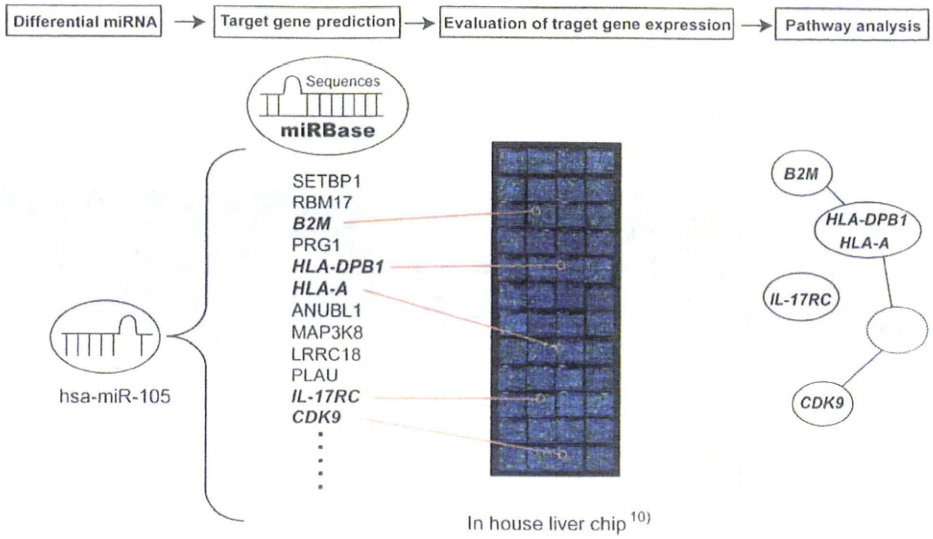

Fig. 4. Analysis of miRNA expression data. Target genes of miRNAs were predicted using MIRANDA Pro3.0; candidate target genes spotted on microarray were identified; number of genes that actually exhibit significant ($P < 0.05$) changes in expression among the genes was determined; and signal pathways involving genes regulated by the miRNAs that had exhibited differential expression between each group were analyzed using MetaCore (Table 4).

noting that the prediction rate may be likely an overestimate of the true rate, given the weaknesses of cross-validation and bootstrapping methods in a strict sense.)

Microarray Analysis. cDNA microarray slides (Liver chip 10k) were used as described.[10] RNA isolation, amplification of antisense RNA, labeling, and hybridization were performed according to the protocols described.[9,10] Quantitative assessment of the signals on the slides was performed by scanning on the ScanArray 5000 (General Scanning, Watertown, MA) followed by image analysis using GenePix Pro 4.1 (Axon Instruments, Union City, CA) as described.[10]

Preliminary Survey of Independency of Paired Samples from the Same Patient. CH and HCC expression data were derived from the same patient. Before further analysis, we examined whether the miRNA expression of paired samples was similar or independent. We compared differences in the expressions of paired and nonpaired CH and HCC samples using the Dunnett test[12] (Supplementary Data). All possible tests performed for data pairs represented no dependency due to the paired data from the same patients. For data analysis, we used the standard pairwise class comparison and prediction tool in BRB ArrayTools.

Identification of Candidate miRNA Target Genes. Candidate target genes predicted to be regulated by miRNAs based on sequence comparison were selected using MIRANDA Pro3.0 (Sanger Institute). Of the selected genes, those represented on a microarray chip were then examined for expression (Fig. 4). The number of genes showing a significant ($P < 0.05$) expression difference among the candidate target genes represented on the chip was statistically analyzed to evaluate the significance of expression regulation by miRNAs. Analysis of significance was performed using Hotelling T2 test (BRB ArrayTools).

Pathway Analysis. Of the candidate miRNA target genes, those showing a significant ($P < 0.01$) expression difference between N, CH-B, HCC-B, CH-C, and HCC-C samples were analyzed for pathways involving these genes using MetaCore software suite (GeneGo, St. Joseph, MI). Significance probability was calculated using

Table 2-1. Class Prediction

No.	Class	Prediction (%)	No. of Predictors	*P* Value
1	HBV versus HCV	87	32	<0.001
2	N versus CH (B+C)	91	26	0.007
3	CH (B+C) versus HCC (B+C)	92	34	0.003

Class prediction algorithm was used for the classification of two groups of patients. Feature selection was based on the univariate significance level (alpha = 0.01). The support vector machine classifier was used for class prediction.

Abbreviations: CH, nontumor lesion of HCC; HCC, hepatocellular carcinoma; N, normal.

Table 2-2 Binary Tree Classification

Node	Group 1 Class	Group 2 Class	No. of Predictors	Misclassification Rate (%)
1	HCC-B, HCC-C, CH-B, CH-C	N	20	4.9
2	HCC-B, CH-B	HCC-C, CH-C	19	13.5
3	HCC-B	CH-B	15	29.2
4	HCC-C	CH-C	14	17.9

Binary tree classification algorithm was used for the classification of each category of patients. Feature selection was based on the univariate significance level (alpha = 0.01). The support vector machine classifier was used for class prediction. There were four nodes in the classfication tree.

Abbreviations: CH-B, non-tumor lesion of HCC-B; CH-C, nontumor lesion of HCC-C; HCC-B, hepatitis B virus-related hepatocellular carcinoma; HCC-C, hepatitis C virus-related hepatocellular carcinoma; N, normal